Molecular Neurobiology (2019) 56:4760–4777
https://doi.org/10.1007/s12035-018-1402-4

Ceramide Induces the Death of Retina Photoreceptors Through Activation of Parthanatos

Facundo H. Prado Spalm[1] · Marcela S. Vera[1] · Marcos J. Dibo[1] · M. Victoria Simón[1] · Luis E. Politi[1] · Nora P. Rotstein[1]

Received: 6 July 2018 / Accepted: 17 October 2018 / Published online: 1 November 2018

Abstract

Ceramide (Cer) has a key role inducing cell death and has been proposed as a messenger in photoreceptor cell death in the retina. Here, we explored the pathways induced by C_2-acetylsphingosine (C_2-Cer), a cell-permeable Cer, to elicit photoreceptor death. Treating pure retina neuronal cultures with 10 μM C_2-Cer for 6 h selectively induced photoreceptor death, decreasing mitochondrial membrane potential and increasing the formation of reactive oxygen species (ROS). In contrast, amacrine neurons preserved their viability. Noteworthy, the amount of TUNEL-labeled cells and photoreceptors expressing cleaved caspase-3 remained constant and pretreatment with a pan-caspase inhibitor did not prevent C_2-Cer-induced death. C_2-Cer provoked polyADP ribosyl polymerase-1 (PARP-1) overactivation. Inhibiting PARP-1 decreased C_2-Cer-induced photoreceptor death; C_2-Cer increased polyADP ribose polymer (PAR) levels and induced the translocation of apoptosis inducing factor (AIF) from mitochondria to photoreceptor nuclei, which was prevented by PARP-1 inhibition. Pretreatment with a calpain and cathepsin inhibitor and with a calpain inhibitor reduced photoreceptor death, whereas selective cathepsin inhibitors granted no protection. Combined pretreatment with a PARP-1 and a calpain inhibitor evidenced the same protection as each inhibitor by itself. Neither autophagy nor necroptosis was involved in C_2-Cer-elicited death; no increase in LDH release was observed upon C_2-Cer treatment and pretreatment with inhibitors of necroptosis and autophagy did not rescue photoreceptors. These results suggest that C_2-Cer induced photoreceptor death by a novel, caspase-independent mechanism, involving activation of PARP-1, decline of mitochondrial membrane potential, calpain activation, and AIF translocation, all of which are biochemical features of parthanatos.

Keywords Photoreceptor death · PARP · Ceramide · AIF · Calpain · Parthanatos

Introduction

Retina neurodegenerative diseases, with diverse etiologies and pathogenesis, are the leading causes of visual dysfunction in developed countries. They include inherited diseases, such as retinitis pigmentosa, which results from over 160 genetic mutations [1], and retinopathies resulting from the combination of environmental risks, genetic predisposition, and old age, such as age-related macular degeneration. The fact that photoreceptor cell death is a hallmark of most of these diseases, irrespective of their origin, makes it imperative to identify common pathways or mediators leading to this death, to develop new therapeutical approaches aimed at providing much needed effective treatments.

In the last two decades sphingolipids have been established as essential players in key cellular functions [2, 3]. Ceramide (Cer) is a central molecule in sphingolipid biosynthetic and catabolic pathways. It can be formed by de novo synthesis, through hydrolysis of phosphodiester bonds in sphingomyelin by sphingomyelinases or through a recycling pathway, by re-acylation of sphingosine [2]. Multiple cellular injuries activate these pathways increasing the levels of Cer, which then triggers different cellular responses, including cell death [2, 4]. The work of several groups, including ours, supports a role for Cer as a mediator of photoreceptor death. Exogenous addition of C_2-acetylsphingosine (C_2-Cer), an extensively used cell-permeable Cer, induces apoptosis of retina neurons in vitro, whereas inhibiting Cer synthesis prevents oxidative stress-induced apoptosis of photoreceptors and of 661W cells, a cone-like cell line [5, 6]. Further evidence points to Cer

Electronic supplementary material The online version of this article (https://doi.org/10.1007/s12035-018-1402-4) contains supplementary material, which is available to authorized users.

✉ Nora P. Rotstein
inrotste@criba.edu.ar

[1] Instituto de Investigaciones Bioquímicas, Depto. de Biología, Bioquímica y Farmacia, Universidad Nacional del Sur (UNS)-CONICET, 8000 Bahía Blanca, Buenos Aires, Argentina

involvement in pathological photoreceptor death in vivo. Cer production has been associated with retinal apoptosis following retinal detachment [7] and suppression of acid sphingomyelinase partially protects the retina from ischemic damage [8]. Cer increases during photoreceptor degeneration in a mouse model of retinitis pigmentosa, and inhibiting its synthesis preserves photoreceptor structure and function [9]. In rat models of retinal degeneration, such as a light stress rat model and P23H-1 rats, inhibiting Cer synthesis with FTY720 grants protection from retina and photoreceptor degeneration [10, 11]. Thus, Cer emerges as a common arbitrator in diverse retinal pathologies, with different etiologies, causing photoreceptor death. This leads to the exciting proposal that targeting either biosynthesis of Cer or the downstream cellular pathways it triggers might provide ubiquitous and effective therapeutical strategies.

Cer has multiple intracellular targets, and mitochondria are a crucial site of Cer-elicited cell death; Cer increase provokes mitochondrial dysfunction and caspase-dependent apoptosis in different cell types [4]. Cer also activates other mechanisms of cell death. Several groups have reported Cer has a role in autophagy induction [12, 13]; increases in Cer levels have been shown to be involved in necroptosis [14]. The pathways leading to an increase in Cer synthesis in the eye differ in the diverse models and pathologies analyzed [5, 6, 8]. Cer increase leads to mitochondrial depolarization in rat photoreceptors and to activation of caspases, calpains and cathepsins in 661W cells [5, 6], suggesting that Cer might control several death pathways in photoreceptors.

Information regarding these pathways is still scarce in the retina, and in vitro models have provided most of the existing data. We established that a 24-h treatment of pure neuronal cultures with 10 μM C_2-Cer induces the death of both photoreceptor and amacrine neurons in culture [5]. In this work, we have determined that a 6-h C_2-Cer treatment triggered the selective death of photoreceptors. Taking advantage of this model, we here investigated the early steps activated exclusively in photoreceptors to induce their degeneration. We have established that C_2-Cer triggers a caspase-independent pathway involving overactivation of poly(ADP ribose) polymerase 1 (PARP-1), activation of calpain, and nuclear translocation of AIF, all of which are established hallmarks of parthanatos, suggesting that this cell death pathway has a key role in Cer-induced photoreceptor death.

Experimental Procedures

Animals

Two-day-old albino Wistar rats bred in our own colony were used in all the experiments. All procedures concerning animal use were carried out in strict accordance with the National Institutes of Health Guide for the Care and Use of Laboratory Animals and following the protocols approved by the Institutional Committee for the Care of Laboratory Animals from the Universidad Nacional del Sur (Argentina).

Materials

Plastic culture 35- and 60-mm diameter dishes as well as 24-multiwell plate (CellStar) were from Greiner Bio-One (Frickenhausen, Germany). Dulbecco's modified Eagle's medium (DMEM), Hanks' Balanced Salt Solution (HBSS), trypsin, gentamicin, terminal deoxynucleotide transferase dUTP nick end labeling (TUNEL) kit, and MitoTracker Red CMXRos were from Invitrogen (Buenos Aires, Argentina). Poly-ornithine, insulin, trypsin inhibitor, transferrin, hydrocortisone, putrescine, trypsin, N-acetyl-D-sphingosine (C_2-ceramide), paraformaldehyde, 4,6-diamidino-2-phenylindole (DAPI), Bafilomycin A1, monoclonal anti-sintaxin-1 (HPC-1) and anti-alpha tubulin antibodies, propidium iodide, and Thiazolyl Blue Tetrazolium Bromide (MTT) were from Sigma-Aldrich (Buenos Aires, Argentina). C16-ceramide (d18:1/16:0, N-palmitoyl-D-erythro-sphingosine) was from Avanti Polar Lipids (Alabaster, Alabama) and a kind gift from Dr. Marta Aveldaño and Dr. Alejandro Peñalva (Bahía Blanca, Buenos Aires, Argentina). Monoclonal anti-AIF (E-1), secondary antibodies, goat anti-mouse IgG-horseradish peroxidase (HRP), z-VAD-FMK, Necrostatin-1, 3-MA, ALLN, Calpeptin, CA-074, Pepstatin A, PJ34, and BYK204165 were from Santa Cruz Biotechnology Inc. (Dallas, Texas). Monoclonal anti-cleaved caspase-3 antibody was from Cell Signaling Technology, Inc. (Danvers, MA), monoclonal anti-PAR antibody from Enzo Life Sciences, Inc. (Miami, FL) and secondary Cy3-conjugated goat anti-rabbit and Cy2-conjugated goat anti-mouse antibodies from Jackson ImmunoResearch (West Grove, PA). Anti-Crx antibody was a generous gift from Cheryl Craft (University of Southern California, Los Angeles, CA). Solvents were HPLC grade, and all other reagents were of analytical grade.

Retinal Neuronal Cultures

Pure neuronal retinal cultures were obtained according to previously established procedures [15]. Briefly, retinas were dissected and dissociated under mechanical and trypsin digestion; cells were then re-suspended in a chemically defined medium and seeded on 24-well cell culture plates or 35/60-mm diameter dishes, according to the experimental design. Culture dishes and wells were pretreated with poly-ornithine (0.1 mg/mL) for 2 h and then with 25% Schwannoma-conditioned medium overnight [16]. Cultures were incubated at 36.5 °C in a humidified atmosphere of 5% CO_2 for 3 days.

Ceramide Addition

C_2-Cer was prepared in ethanol, as a 25-mM stock solution, and then added to neuronal cultures at day 3 in vitro at a final concentration of 10 μM C_2-Cer [5]. The same volume of solvent was added to control cultures (0.04% ethanol [*v*/*v*]). Different time periods (3, 6, and 9 h) were tested initially and a 6-h treatment was chosen for further experiments, unless otherwise specified.

The effect of C16-Cer on cultured neurons was also analyzed. A 4-mg/mL (7.41 mM) C16-Cer stock solution was prepared in ethanol/decane (98:2 *v*/*v*), to allow its entrance to the cell. The solution was added to the cultures at 5, 10, 15, 20 and 25 μM (final concentration in culture) [17] and neurons were incubated for 6 h. The same volume of solvent was added to control conditions (maximum solvent concentration, 0.33% ethanol/decane, *v*/*v*).

Cell Treatment Protocols

To evaluate the effect of different inhibitors on C_2-Cer-induced cell death, cultures were pretreated with each inhibitor for 1 h before C_2-Cer addition. A detailed description of the inhibitors used is shown in Table 1. To evaluate the effect of PJ34 pretreatment on C16-Cer-supplemented cultures, neuronal cultures were pretreated with 1 μM PJ34 for 1 h and then with different concentrations of C16-Cer for 6 h.

For immunocytochemical analyses, cultures were fixed for 30 min with 2% paraformaldehyde (PF, Sigma) in phosphate-buffered saline (PBS), or with cold methanol at − 20 °C for 15 min, followed by permeation with 0.1% Triton X-100 for 15 min. Non-specific labeling was blocked by 1 h incubation at room temperature (RT) with 2% skimmed milk in TNT buffer (100 mM Tris pH 7.4; 150 mM NaCl and 0.1% Tween 20).

Evaluation of Neuronal Cell Death

Cell death was determined by propidium iodide (PI) labeling. Cultures were incubated with 25 μM PI for 20 min at 36.5 °C and then washed twice with PBS before fixation. PI-labeled cells were considered non-viable [18].

Cell viability and mitochondrial function were evaluated by using 2-(4,5-dimethylthiazol-2-yl)-2,5-diphenyltetrazolium bromide (MTT) assay [19]. Viable cells reduced MTT to a colored, water-insoluble formazan salt. After treatment, MTT solution (5 mg/ml in PBS) was added to achieve a 0.5 mg/ml MTT final concentration in the culture medium. Cells were incubated at 36.5 °C for 1.5 h, lysed with solubilization buffer (10% Triton X-100 and 0.01 N HCl in isopropanol), and the extent of MTT reduction was measured spectrophotometrically at 570 nm using a microplate reader. Background absorbance (due to phenol red of DMEM) was measured at 670 nm and subtracted for all wells. Viability is expressed as a percentage of the average absorbance of controls.

Preservation of mitochondrial membrane potential was determined incubating the cultures with 100 nM MitoTracker Red CMX ROS (Molecular Probes, Invitrogen) at 36.5 °C for 20 min before fixation. Cell labeling was then analyzed by fluorescence microscope (Nikon Eclipse 2000). MitoTracker concentrates in mitochondria retaining their membrane potential, labeling them with a bright red fluorescence; in contrast, a diffuse, pale red labeling is observed upon mitochondrial depolarization [20]. After incubation, cells were gently washed with PBS and fixed with 2% PF for 30 min.

Nuclear integrity was evaluated by labeling nuclei with 1 μg/ml DAPI for 10 min. Apoptotic cell death was evaluated by the TUNEL assay. Cells were fixed with 2% PF for 15 min and stored in 70% ethanol for 48–72 h at − 20 °C. Cells were then pre-incubated with TdT buffer for 15 min and then with the TdT reaction mixture (0.05 mM BrdUTP and 0.3 U/μL recombinant TdT in TdT buffer) at 36.5 °C in a humidified atmosphere for 1 h. The reaction was stopped with stop buffer (300 mM NaCl, 30 mM sodium citrate, pH 7.4) at room temperature. Negative controls were prepared by omitting the enzyme TdT. BrdU uptake was determined with an anti-BrdU monoclonal antibody.

Plasma membrane leakage, a feature shared by both necrosis and necroptosis, was determined by detection of the release of lactate dehydrogenase (LDH), a cytoplasmic enzyme, to culture media. LDH leakage was determined as described by Sanchez Campos et al. [21] with slight modifications. After C_2-Cer treatment, incubation media were removed and cells centrifuged at 1000×*g* for 10 min at 4 °C. LDH activity was measured in the supernatant, by a spectrophotometrical assay (LDH-P UV AA kit, Wiener lab, Argentina). In this assay, the conversion rate of reduced nicotinamide adenine dinucleotide (NADH) to oxidized nicotinamide adenine dinucleotide (NAD^+), reaction catalyzed in presence of LDH, was followed at 340 nm. Results were expressed as percentage of the control.

Determination of Reactive Oxygen Species (ROS) Levels

ROS levels were evaluated using the probe 2′,7′-dichlorodihydrofluorescein diacetate (H2-DCFDA, DCF) (Thermo Fisher). This probe can cross the membrane and after oxidation is converted into a fluorescent compound. After a 4-h C_2-Cer treatment, media was removed, and PBS buffer containing 1 μM DCF was added. After 20 min of incubation at 36.5 °C, cell labeling was analyzed using an epifluorescence microscope. Neuronal cultures treated with 350 μM hydrogen peroxide for 6 h were used as positive controls; dishes containing culture media, without cells, were used as negative controls. Fluorescence levels were quantified using ImageJ (freely

Table 1 List of inhibitors

Inhibitor	Source	Stock solution	Concentrations tested	Maximum solvent concentration (% *v/v*)
3-MA	Santa Cruz (sc-205596)	200 mM (DMEM)	100, 250, 500, and 1000 μM	–
ALLN	Santa Cruz (sc-221236)	26.1 mM (DMSO)	10, 20, and 50 μM	0.19
Bafilomycin A1	Sigma # B1793	20 μM (DMSO)	1, 10, and 100 nM	0.05
BYK204165	Santa Cruz (sc-214642)	66.7 mM (DMSO)	2.5, 5, and 10 μM	0.02
CA-074	Santa Cruz (sc-214647)	16.8 mM (DMSO)	1, 5, and 10 μM	0.06
Calpeptin	Santa Cruz (sc-202516)	14 mM (DMSO)	0.5, 1, and 2.5 μM	0.02
Necrostatin-1	Santa Cruz (sc-200142)	38.5 mM (DMSO)	10, 50, and 100 μM	0.26
Pepstatin A	Santa Cruz (sc-45036)	7.29 mM (DMSO)	1, 5, and 10 μM	0.14
PJ34	Santa Cruz (sc-204161)	30.4 mM (DMSO)	0.5, 1, 2.5, and 5 μM	0.02
z-VAD-FMK	Santa Cruz (sc-311561)	21.4 mM (DMSO)	10, 20, and 50 μM	0.23

The source, stock solutions, concentrations, and final solvent concentration in the incubation media of the different inhibitors tested are listed

available at http://rsb.info.nih.gov/ij). Results were expressed as a percentage of the control.

Immunocytochemical Analysis

Neuronal cell types were identified by their morphology using phase contrast microscopy and by immunocytochemistry. Photoreceptors were identified by their labeling with an antibody against Crx (1:600, overnight, 4 °C), the transcription factor expressed when progenitor cells begin to differentiate as photoreceptors, and amacrine neurons with an HPC-1 antibody (1:200, 2 h); a Cy3 goat anti-rabbit and a Cy2 anti-mouse (1:200, 1 h) were used as secondary antibodies, respectively. Photoreceptors have a small (3–5 μm) round and dark cell body usually with a single neurite at one end, which usually ends in a conspicuous synaptic "spherule." Amacrine neurons have multiple neurites, instead of a typical single axon, a bigger cell body (around 10 μm), and a broad morphological heterogeneity. The remaining neuronal cell types in culture accounted for less than 5% of total cells.

Activation of caspase-3 was determined by incubating cells with a cleaved caspase-3 antibody (1:200 overnight, 4 °C); a Cy3 goat anti-rabbit was used as a secondary antibody.

To evaluate AIF nuclear translocation, cells were fixed with methanol and incubated with an anti-AIF antibody (1:50 overnight, 4 °C). A Cy2 goat anti-mouse was used as a secondary antibody. Nuclei were labeled with TOPRO-3 (Invitrogen, 2 μM, 10 min) and samples were analyzed by laser scanning confocal microscopy (DMIRE2/TSCSP2 microscope; Leica, Wetzlar, Germany) with a 63× water objective and processed (LCS software; Leica).

Production of PAR Polymers

PARP-1 activation was analyzed by evaluating production of PAR polymers, by immunocytochemistry and Western blot. For immunocytochemical analysis, cells were incubated with an anti-PAR antibody (1:50, overnight at 4 °C); Cy2 anti-mouse (1:200, 90 min) was used as a secondary antibody. To eliminate unspecific labeling, cells were then washed twice for 10 min with 0.1% Tween in PBS (PBST) and once with PBS.

For Western blotting, cells were rinsed twice with washing buffer (10 mM NaF, 1 mM Na_3VO_4 in PBS), collected in lysis buffer [10 mM Tris-HCl (pH 7.4), 15 mM NaCl, 5 mM NaF, 1 mM Na_3VO_4, 1% Triton X-100] containing a protease inhibitor mixture (Sigma #P8340) and scrapped followed by lysis on ice for 30 min (with vigorous vortexing every 10 min). After quantification of proteins by Bradford assay, 30–40 μg of sample were mixed with sample buffer [62.5 mM Tris-HCl (pH 6.8), 2% SDS, 1% glycerol, 3% 2-mercaptoethanol, and 0.01% bromophenol blue], then heated for 7 min at 95 °C, and finally were subjected to electrophoresis on 10% SDS-PAGE [22]. Proteins were then electro-transferred to Immobilon-FL transfer membranes (PVDF) [Merck Millipore, Burlington, USA] and blocked in PBS buffer containing 5% skim milk or 3% BSA (as necessary) for 2 h at RT. Membranes were then incubated with specific primary antibodies against tubulin (1:1000) and PAR (1:400). After three washes with TBS plus 0.1% Tween (TBST), membranes were incubated with horseradish peroxidase-conjugated goat anti-mouse antibody in TBST for 1 h at RT, washed three times with TBST, and then visualized using an enhanced chemiluminescent technique (ECL), according to the manufacturer's instructions. Images were obtained by scanning at 1200 dpi. Band semi-quantification was carried out using the ImageJ software.

Statistical Analysis

Statistical analysis was performed using ANOVA, followed by the Tukey's multiple-comparison test. Data are shown as mean ± S.E.M. of at least three independent experiments. Differences were considered significant at $p < 0.05$ (*), (#); $p < 0.01$ (**); and $p < 0.001$ (***), (###). When relevant, non-significant differences between conditions were indicated as *ns*.

Results

Cer Rapidly Triggered Selective Photoreceptor Cell Death in Culture

We previously showed that a 24-h treatment with C_2-Cer induces the death of photoreceptors and amacrine neurons in 3-day cultures [5]. To evaluate whether both neuronal types had a differential sensitivity to C_2-Cer, we analyzed its effect after shorter treatments. C_2-Cer induced a rapid increase in neuronal death. PI-labeled (dead) neurons increased markedly after a 6-h treatment with 10 μM C_2-Cer (Fig. 1a, right column). The percentage of PI-labeled neurons significantly increased from less than 10% in controls to 33, 57, and 73% after 3, 6, and 9 h of C_2-Cer treatment, respectively (Fig. 1b).

Similarly, a 6 h C_2-Cer treatment increased neuronal pyknotic nuclei (Fig. 1a, right column, arrowheads), which were very few in controls. The percentage of neurons having pyknotic nuclei rapidly increased from around 10% in controls to 37, 49, and 55% after 3, 6, and 9 h of C_2-Cer treatment, respectively (Fig. 1d). Neuronal mitochondria functionality was already affected after a 6-h C_2-Cer treatment; while most neurons in controls showed brightly labeled (functional) mitochondria (Fig. 1e, left column), a remarkable loss of mitochondrial fluorescence was observed in C_2-Cer-treated cultures (Fig. 1e, right column, thin arrows). MTT assays (Fig. 1f) corroborated that neuronal viability significantly and progressively decreased to about 80, 70, and 50% after 3, 6, and 9 h of C_2-Cer treatment, respectively.

As stated above, C_2-Cer elicits photoreceptor and amacrine neuron death after 24 h. In contrast, a 6-h treatment with C_2-Cer only affected photoreceptors. Few photoreceptors and amacrine neurons, identified by their Crx and HPC-1 labeling, respectively, had pyknotic nuclei in controls (arrowheads in Fig. 2a, upper panel), whereas in C_2-Cer-treated cultures the amount of photoreceptors with pyknotic nuclei remarkably increased (arrowheads in Fig. 2a, lower panel), from less than 15% to about 45% of photoreceptors (Fig. 2b). On the contrary, C_2-Cer treatment did not affect amacrine neurons, which preserved intact nuclei (broken arrows in Fig. 2a); the percentage of these neurons having pyknotic nuclei remained at 10% in both control and C_2-Cer-treated cultures (Fig. 2b). Taking advantage of this selectivity, we chose a 6-h incubation time for further investigating the pathways leading to photoreceptor death.

Noteworthy, analysis of TUNEL labeling of neuronal cells revealed almost no increase in TUNEL-labeled cells after a 6-h C_2-Cer treatment compared to controls (thin arrows in Fig. 3a, first column), which remained at around 5% in both control and C_2-Cer-treated cultures, even 15 h after C_2-Cer addition (Fig. 3b). A double-staining analysis, with an antibody against Crx, revealed that almost no TUNEL-labeled cells were Crx positive (Fig. 3a, third column).

C_2-Cer Increased Reactive Oxygen Species Formation in Photoreceptors

Mitochondria are a main target of Cer, which usually affects their functionality and membrane polarization. The impairment in mitochondrial function leads to an increased ROS formation, which might then activate different cell death pathways. Hence, we explored whether Cer treatment rapidly induced ROS production. Evaluation of ROS levels in neuronal cultures using the DCF fluorescent probe evidenced a remarkable increase in DCF-labeled cells in C_2-Cer-treated cultures compared to controls (Fig. 3c). Whereas controls showed few and diffusely labeled photoreceptors, their number increased, together with a significant increase in fluorescence intensity, after 4 h of C_2-Cer treatment (Fig. 3c, d).

Cer-Induced Photoreceptor Death Is Caspase Independent

As shown in Fig. 1e, C_2-Cer treatment induced the loss of mitochondrial membrane permeability, a central event in triggering cell death. In the "intrinsic apoptotic pathway," this leads to the formation of the apoptosome and the subsequent cleavage and activation of caspase-3. However, immunocytochemical analysis revealed no differences in cells showing cleaved caspase-3 labeling in control and C_2-Cer-treated cultures (Fig. 4a, central column). Only about 5% of the cells showed cleaved caspase-3 labeling both in controls and Cer-treated cultures after 6 h; even after a 15-h treatment, their increase was non-significant compared to controls (Fig. 4b), suggesting that caspase-3 did not participate in C_2-Cer-induced death.

To investigate whether other caspases were involved in this death, cultures were pretreated with the pan-caspase inhibitor z-VAD-FMK. After 6 h of C_2-Cer h treatment, z-VAD-FMK concentrations ranging from 10 to 50 μM did not prevent the decrease in viability induced by C_2-Cer (Fig. 4c), implying that C_2-Cer-induced death was caspase-independent.

PARP-1 Overactivation Is Involved in Cer-Induced Photoreceptor Death

Overactivation of PARP-1 has been shown to promote a caspase-independent form of cell death named parthanatos. To evaluate whether PARP-1 was involved in photoreceptor death, we pretreated neuronal cultures with PJ34, a cell-permeable and highly specific PARP-1 inhibitor, before C_2-Cer addition. Pretreatment with 1 μM PJ34 significantly reduced cell death, as shown by MTT assay (Fig. 5a). Pretreatment with 5 μM BYK, a potent and selective PARP-1 inhibitor, also led to a significant decrease in C_2-Cer-induced photoreceptor death (Fig. 5b). PJ34 pretreatment markedly reduced the nuclear pyknosis provoked by C_2-Cer (arrowheads in Fig. 5c). This pretreatment significantly diminished the increase in the

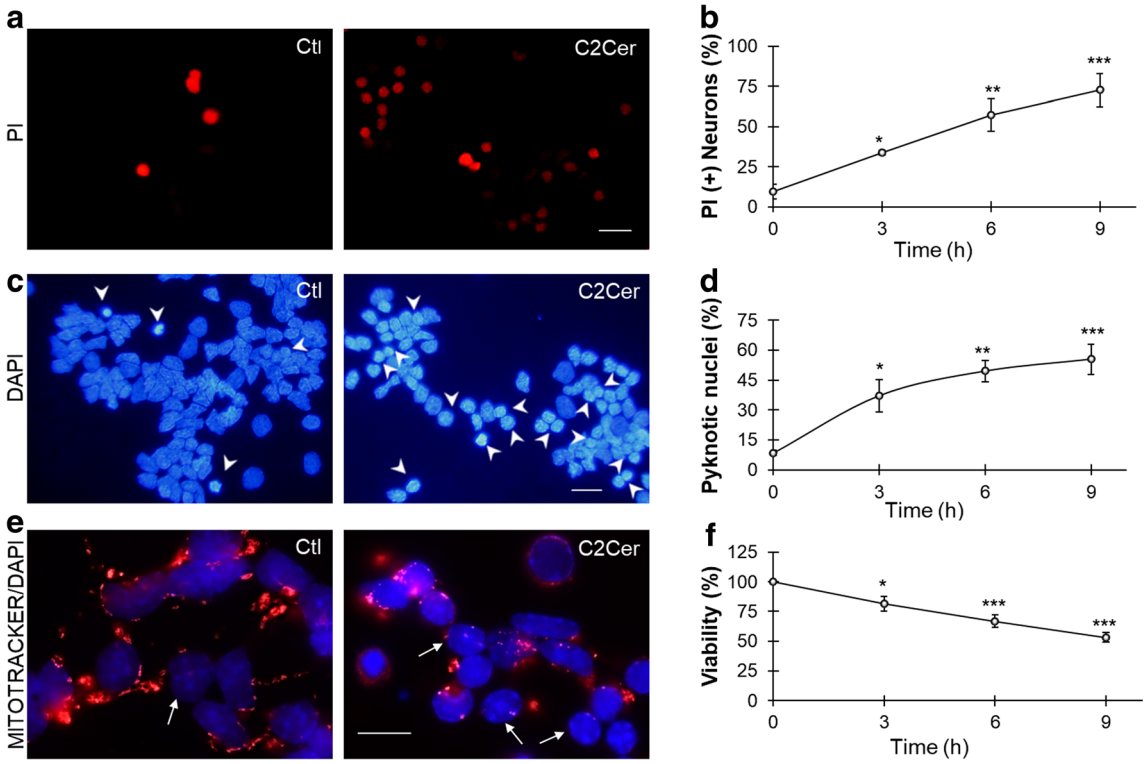

Fig. 1 C_2-ceramide rapidly induced neuronal death. Three-day neuronal cultures were supplemented with vehicle (Ctl) or with 10 μM C_2-Cer (C_2-Cer) for different time periods in culture. Fluorescence photomicrographs show cells labeled with propidium iodide (PI, red in **a**), nuclei labeled with DAPI (blue in **c** and **e**), and mitochondria labeled with MitoTracker (red in **e**) after a 6-h treatment with vehicle or with C_2-Cer; note the increase in neurons having pyknotic nuclei (arrowheads in **c**) and in neurons evidencing mitochondrial depolarization (thin arrows in **e**) in C_2-Cer-treated cultures. Scale bar, 10 μm. Graphs show the percentage of PI-labeled neurons (**b**), of neurons having pyknotic nuclei (**d**), and of decrease in viability compared to controls, determined by MTT assay (**f**) after different times in culture. Values in **b**, **d**, and **f** are the mean ± SEM of three different experiments. *$p < 0.05$; **$p < 0.01$; ***$p < 0.001$, statistically significant differences compared to controls

percentage of photoreceptors with pyknotic nuclei induced by C_2-Cer compared to controls (Fig. 5d).

Overactivation of PARPs, mainly that of PARP-1, leads to a rapid accumulation of polyADP ribose (PAR) polymers. Immunocytochemical labeling demonstrated that C_2-Cer increased PAR expression compared to controls (Fig. 5e). Western blot analysis confirmed that C_2-Cer rapidly increased PAR levels. A strong PAR labeling was observed, stretching between 150 and 240 kDa, in a smear-like fashion. After 2 h of C_2-Cer addition, PAR levels augmented nearly by 50%, compared to controls (Fig. 5f), decreasing after 4 h and increasing slightly, although non-significantly, after 6 h. As a whole, these results strongly support that a rapid PARP overactivation was involved in photoreceptor death.

C16-Cer-Induced Neuronal Death Was Prevented by Inhibiting PARP

We previously showed that oxidative stress increases neuronal synthesis of [^{3}H]16:0-Cer and this increase leads to photoreceptor death [5]. Hence, we evaluated whether C16-Cer, a biological ceramide, also induced neuronal death through the activation of PARP-1. A 6-h treatment with 10 to 25 μM C16-Cer markedly decreased neuronal viability (Fig. 5g). Pretreatment with 1 μM PJ34 significantly augmented this viability (Fig. 5g), suggesting that PARP-1 activation was involved in C16-Cer-induced neuronal death.

C_2-Cer-Induced PARP-1 Activation Led to AIF Nuclear Translocation

AIF is among the "death factors" released from mitochondria upon different death signals that lead to the loss of mitochondrial membrane permeability and its nuclear translocation has a deadly effect [23]. To explore whether C_2-Cer-induced AIF nuclear translocation, AIF localization was evaluated by immunocytochemistry and confocal microscopy. Double labeling with an AIF (green in Fig. 6a) antibody and TOPRO-3 (blue in Fig. 6a) evidenced that AIF was almost absent from nuclei in controls; in contrast, C_2-Cer enhanced AIF and TOPRO-3 colocalization in neuronal nuclei, implying it promoted AIF nuclear translocation (compare left and right micrographs in

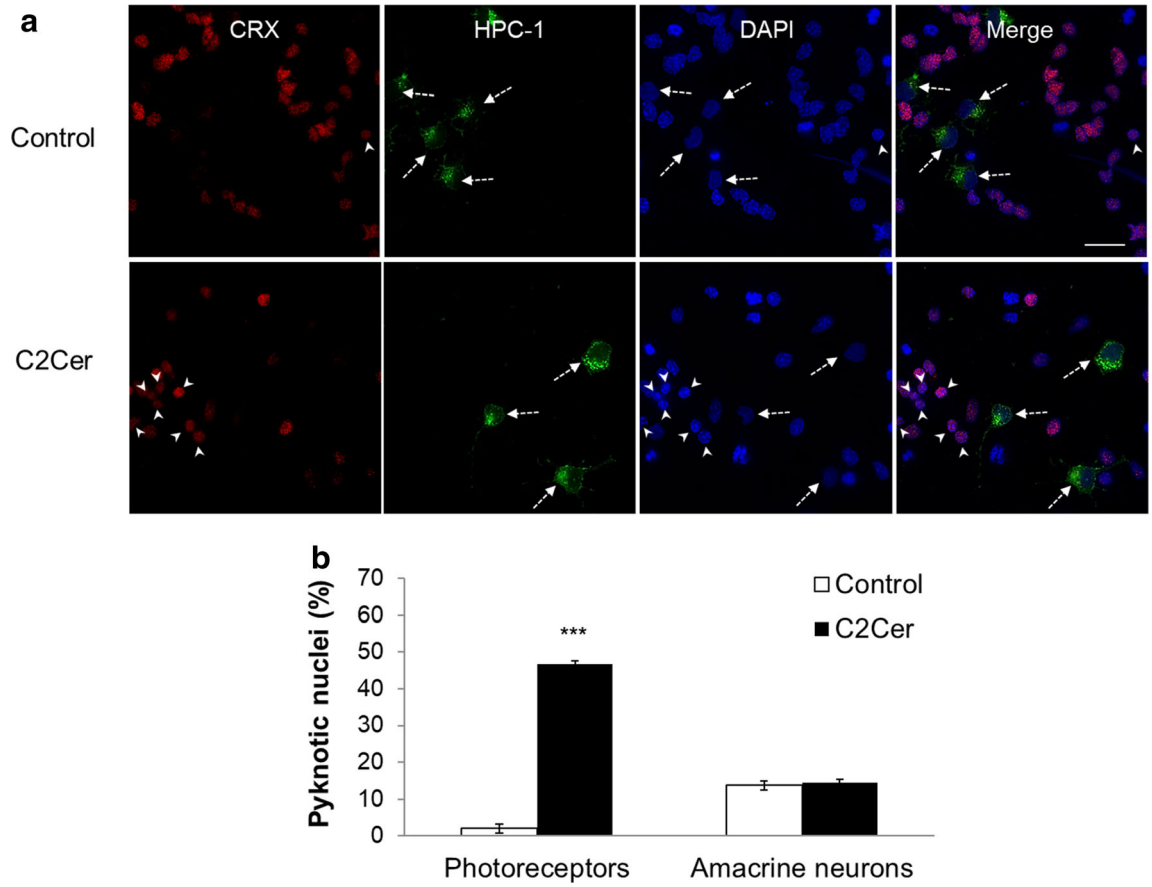

Fig. 2 A 6-h treatment with C_2-Cer induced the selective death of photoreceptors. Cultures were treated with vehicle (control) or with C_2-Cer for 6 h. **a** Fluorescence photomicrographs show photoreceptors and amacrine neurons labeled with Crx (red) and HPC-1 (green, broken arrows) antibodies, nuclei labeled with DAPI (blue), and merge. Arrowheads indicate Crx-labeled photoreceptors having pyknotic nuclei. Scale bar, 10 μm. **b** Bars show the percentage of photoreceptors and amacrine neurons, identified as shown in **a**, having pyknotic nuclei in controls and C_2-Cer-treated cultures; values are the mean ± SEM of three different experiments. ***$p < 0.001$, statistically significant differences compared to controls

Fig. 6a, upper lane, arrowheads). Evaluation of AIF nuclear localization by confocal imaging analysis in the xz plane confirmed the absence of AIF in nuclei in controls and its nuclear translocation after C_2-Cer treatment, as evidenced by the colocalization of AIF and TOPRO-3 labeling (Fig. 6b, first and third lanes, respectively). The percentage of neurons showing AIF nuclear localization increased from about 20% in controls to 60% after 6 h of C_2-Cer treatment (Fig. 6c).

PARP-1-mediated cytotoxicity has AIF as a central effector in many cell types [24–26]. To evaluate whether AIF nuclear translocation resulted from PARP-1 overactivation, we pretreated neuronal cultures with PJ34. This PARP-1 inhibitor noticeably decreased AIF nuclear translocation after C_2-Cer treatment (Fig. 6a, lower lane). This decrease was confirmed by analysis on the xz plane; scarce AIF and TOPRO-3 colocalization was observed in PJ34-pretreated cultures, compared to those solely treated with C_2-Cer (Fig. 6b, third and fourth lanes, respectively). The percentage of neurons showing AIF nuclear localization significantly decreased from 60% to about 20% in C_2-Cer-treated cultures without or with PJ34 pretreatment, respectively (Fig. 6c).

C_2-Cer Induced Calpain Activation to Promote Photoreceptor Death

Cysteine proteases such as calpains and cathepsins participate in AIF cleavage, which is essential for its translocation [27, 28]; however, the requirement for their activation in PARP-1-mediated death is still under debate [26, 29]. We first analyzed the effect of ALLN, an inhibitor of several cysteine proteases, such as calpain 1 and 2 and cathepsins B and L. ALLN pretreatment remarkably preserved neuronal viability. Pretreatment with 20 μM ALLN, 1 h before C_2-Cer treatment, markedly reduced the nuclear pyknosis observed in C_2-Cer-

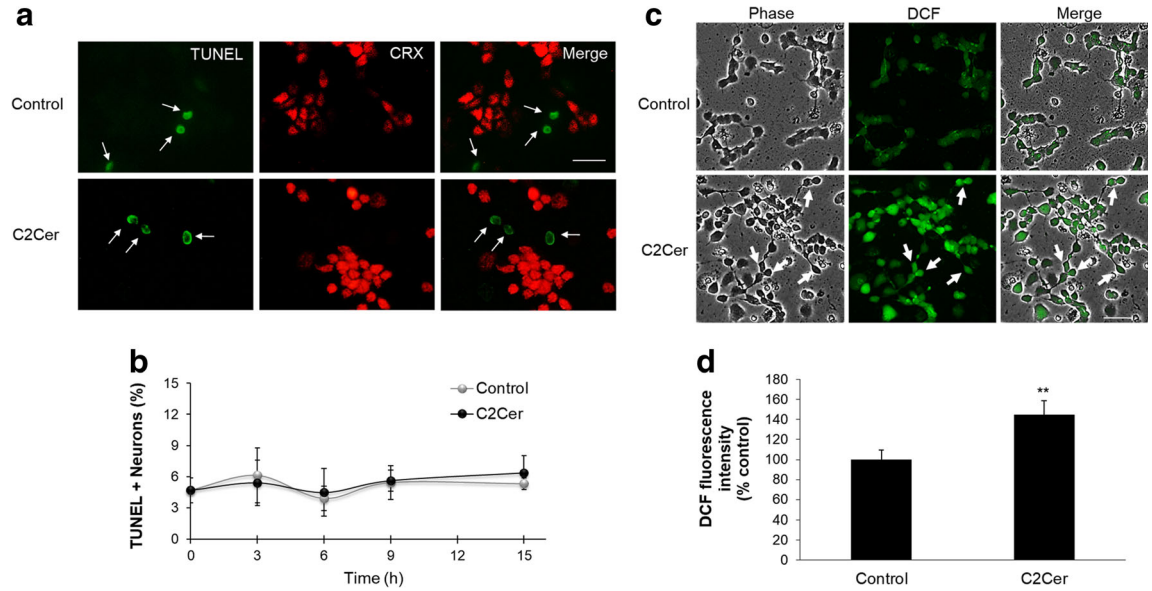

Fig. 3 C_2-Cer enhanced the formation of reactive oxygen species (ROS) but did not increase DNA internucleosomal fragmentation. **a** Fluorescence photomicrographs show cultures treated with vehicle or with C_2-Cer for 6 h, labeled with TUNEL (green, thin arrows), to evaluate DNA internucleosomal fragmentation, a characteristic of apoptosis, Crx (red), to identify photoreceptors, and merge. Note the lack of colocalization of TUNEL labeling and Crx expression in the merge images. **b** Percentage of TUNEL-positive neurons after different times in culture. **c** Phase and fluorescence micrographs show cultures treated with vehicle or with C_2-Cer for 4 h, labeled with DCF, to detect formation of ROS (green), and merge; thick white arrows indicate ROS formation in photoreceptors. **d** Bars depict the percentage of increase, in arbitrary units of fluorescence intensity, in C_2-Cer-treated cultures compared to controls; $^{**}p < 0.01$, statistically significant differences compared to controls. Scale bars, 20 μm

treated cultures (Fig. 7a, compare central and right micrographs; b). ALLN pretreatment maintained 80% viability, compared to controls, preventing the 50% decrease induced by C_2-Cer (Fig. 7c). This implies that either calpains or cathepsins, or both, were involved in C_2-Cer-induced photoreceptor death.

We then pretreated the cultures with different concentrations of calpeptin, a potent calpain I and II inhibitor, before C_2-Cer addition. MTT assays showed that 1 μM calpeptin significantly preserved neuronal viability upon C_2-Cer treatment (Fig. 7d). Calpeptin decreased nuclear pyknosis in photoreceptors compared to the observed in C_2-Cer-treated cultures (Fig. 7e, arrowheads; f). Noteworthy, ALLN neuroprotection was more effective than that of calpeptin.

Finally, we investigated whether PARP-1 and calpains acted additively or synergically to trigger photoreceptor death. We simultaneously inhibited PARP-1 and calpain activation by supplementing the cultures with both 1 μM PJ34 and 1 μM calpeptin before C_2-Cer treatment. This combined treatment had the same protective effect as PJ34 alone and slightly higher than that of calpeptin (Fig. 7g). This suggests that PARP-1 and calpain are acting through the same pathway to protect photoreceptors from C_2-Cer-induced death.

Inhibiting cathepsins had no effect on neuronal viability. MTT assays showed that pretreatment of neuronal cultures with 1–10 μM CA-074, a selective cathepsin B inhibitor, and 5–10 μM pepstatin A, an inhibitor of acidic proteases such as cathepsin D, failed to prevent C_2-Cer-induced reduction in neuronal viability (Supplementary Fig. 1).

Since calpains have been reported to cleave AIF and promote its translocation, we evaluated the effect of calpeptin pretreatment on AIF translocation. Colocalization of AIF and TOPRO-3 labeling (arrowheads in Fig. 8a) was highly visible in C_2-Cer-treated cultures and markedly decreased when cultures were pretreated with calpeptin. The increased colocalization after C_2-Cer treatment and its decrease with calpeptin pretreatment were clearly appreciated when AIF and TOPRO-3 labeling were analyzed in the xz plane (Fig. 8b, merge in third and fourth lane, respectively). Quantitative analysis confirmed that calpeptin pretreatment reduced C_2-Cer-induced AIF translocation (Fig. 8c). As a whole, these data suggest that calpains participated in photoreceptor death induced by C_2-Cer and were involved in AIF nuclear translocation.

PARP-1 has been implicated as a player in other caspase-independent death pathways such as necroptosis and autophagy. Necroptosis is characterized by the loss of plasma membrane integrity, as occurs in necrosis, following a program orchestrated by the death domain receptor-associated adaptor kinase 1 (RIPK1). LDH leakage, which results from the loss of plasma membrane integrity, was similar in controls and in C_2-Cer-treated cultures (Supplementary Fig. 2A).

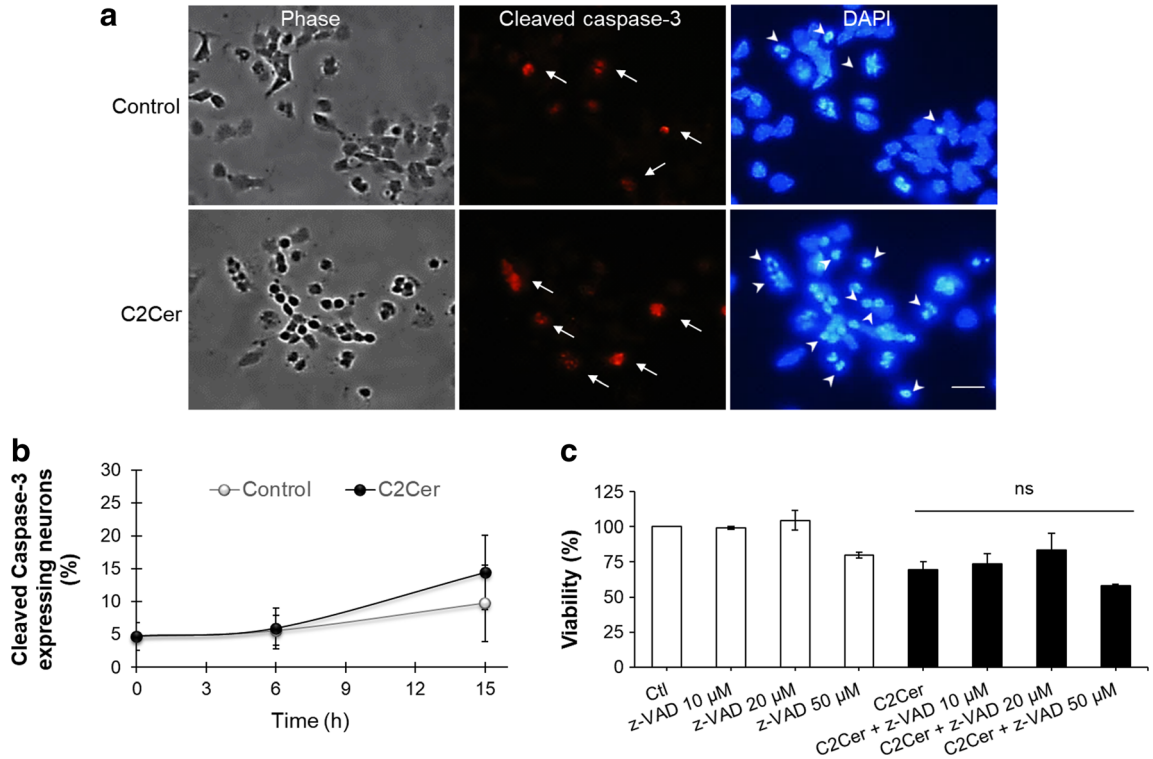

Fig. 4 C_2-Cer induced cell death by a caspase-independent pathway. **a** Phase and fluorescence photomicrographs of cultures treated with vehicle or with C_2-Cer for 6 h showing expression of cleaved caspase-3 (middle column, arrows) and nuclei labeled with DAPI (right); arrowheads show pyknotic nuclei. Scale bar, 10 μm. **b** Percentage of cells showing the presence of cleaved caspase-3 after different times of C_2-Cer addition. **c** Bars depict the effect on neuronal viability, compared to controls, of pretreatment with different concentrations of pan-caspase inhibitor z-VAD-FMK (z-VAD), followed (black bars) or not (white bars) by a 6-h C_2-Cer treatment. ns, non-significant statistical differences

Pretreatment with necrostatin-1, a potent RIPK1 inhibitor, in concentrations ranging from 10 to 100 μM, did not reduce C_2-Cer-induced cell death (Supplementary Fig. 2B).

PARP-1 plays dual roles in the modulation of parthanatos and autophagy under oxidative stress [30]. Evaluation of the possible role of autophagy in C_2-Cer-induced photoreceptor death showed that pretreatment with 100–1000 μM 3-MA, an autophagy inhibitor, failed to prevent C_2-Cer-induced cell death (Supplementary Fig. 2C). Similarly, pretreatment with 0.1–10 nM Bafilomycin A1, another autophagy inhibitor, did not preserve neuronal viability after C_2-Cer treatment (Supplementary Fig. 2D). As a whole, these results imply that neither programmed necrosis nor autophagy participates in the demise of photoreceptors following C_2-Cer treatment and PARP-1 activation.

Discussion

Cer accretion emerges as a common feature during retina neurodegeneration, leading to the death of photoreceptors. However, the pathways leading to this death are still ill-defined. We here provide evidence for a novel pathway activated by Cer in photoreceptors to trigger their death. We demonstrated that treatment with 10 μM C_2-Cer for 6 h induced the selective death of cultured retina photoreceptors through a caspase-independent pathway. This death involved ROS generation, activation of PARP-1, accumulation of PAR, activation of calpains, the loss of mitochondrial membrane potential, and translocation of AIF, all of which are features characterizing a recently established cell death pathway named parthanatos. Hence, our results suggest that C_2-Cer elicited photoreceptor death by activating parthanatos as the cell death routine.

Accumulating evidence in animal models of diverse retinal pathologies supports a role for Cer as a key mediator triggering photoreceptor death. Cer levels are increased in the retinas of animal models of retinal degeneration; Cer accumulates during retina degeneration in an animal model of retinitis pigmentosa, and inhibiting its synthesis delays both rod and cone photoreceptor death and preserves visual function [9, 31]. Light stress induces Cer de novo synthesis and retina degeneration involving photoreceptor death, and prevention of this synthesis protects retina structure and function [10]. Ischemia provokes an increase in Cer levels due to activation of acid sphingomyelinase (ASMase) and the resulting retina damage is reduced in ASMase +/- mice [8]; Cer accumulates at early stages during degeneration of P23H-1 rat retinas [11]. In an early work we established that oxidative stress increases Cer synthesis in retina neurons in culture and a 24-h treatment

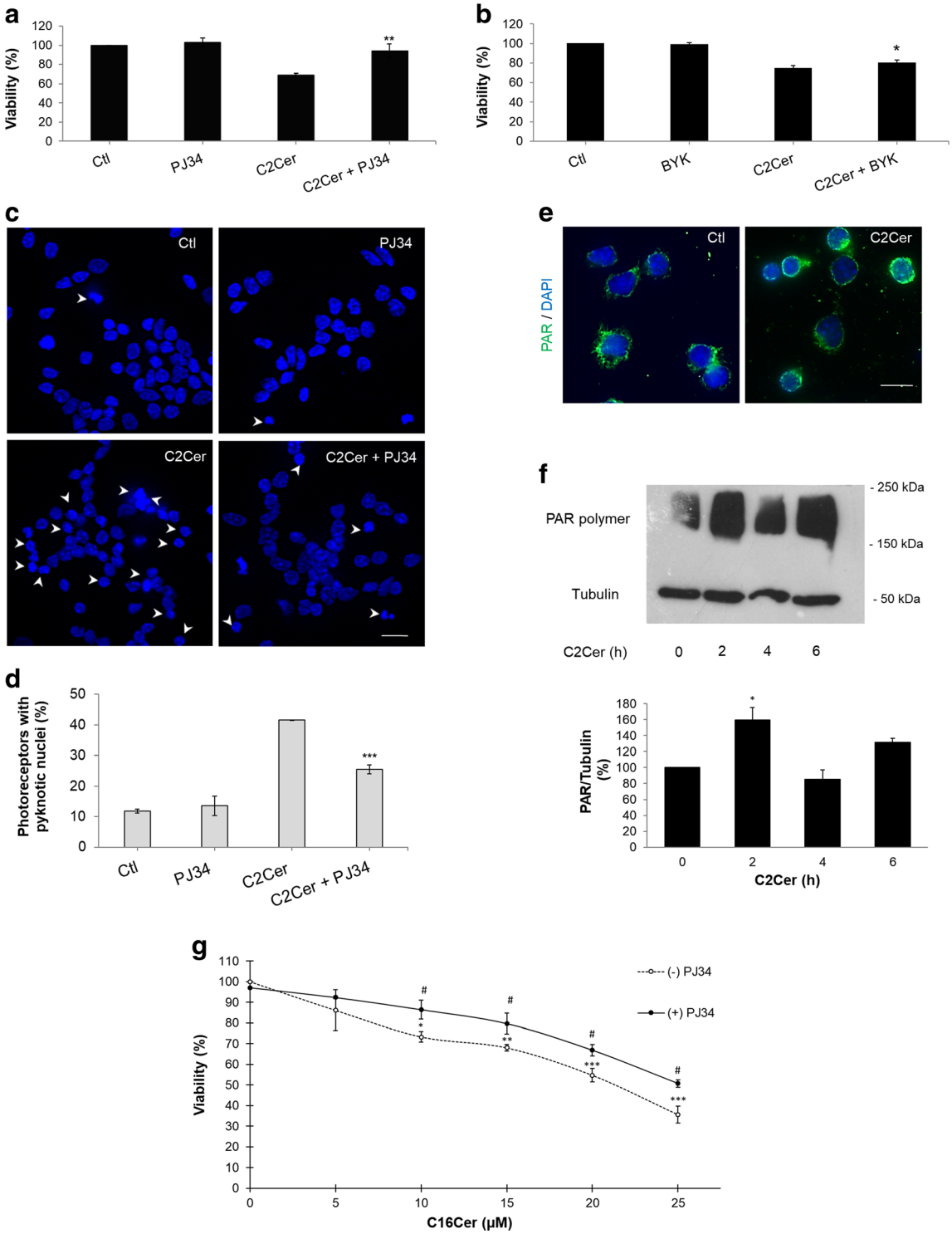

Fig. 5 C_2-Cer promoted neuronal death through activation of PARP-1. **a**, **b** Cultures were pretreated with different concentrations of two PARP-1 inhibitors, PJ34 and BYK, respectively, before a 6-h treatment with C_2-Cer; viability was then determined by MTT assays. **c** Fluorescence photomicrographs show nuclei labeled with DAPI in cultures pretreated with 1 μM PJ34 and then with vehicle or with C_2-Cer for 6 h; arrowheads show pyknotic nuclei. **d** Bars show the percentage (mean ± SEM) of photoreceptors having pyknotic nuclei in controls and cultures pretreated with PJ34, with or without a 6-h C_2-Cer treatment. **e** Photomicrographs show expression of PAR polymers (green) and nuclei labeled with DAPI (blue) in cultures treated with vehicle or with C_2-Cer for 2 h. Scale Bars, 10 μm. **f** Analysis by Western blot of the levels of PAR polymers at 0, 2, and 4 h of C_2-Cer addition (up); bars depict the percent of change in normalized PAR polymer levels, compared to control condition (time zero). **g** The curves show the viability (as mean percentage ± SEM), determined by MTT assays, of neurons pretreated with (•) or without (○) PJ34 and then with different concentrations of C16-Cer for 6 h. $^{*}p < 0.05$, $^{**}p < 0.01$, $^{***}p < 0.001$, statistically significant differences compared to controls; $^{\#}p < 0.05$, statistically significant differences between PJ34-treated and non-treated conditions

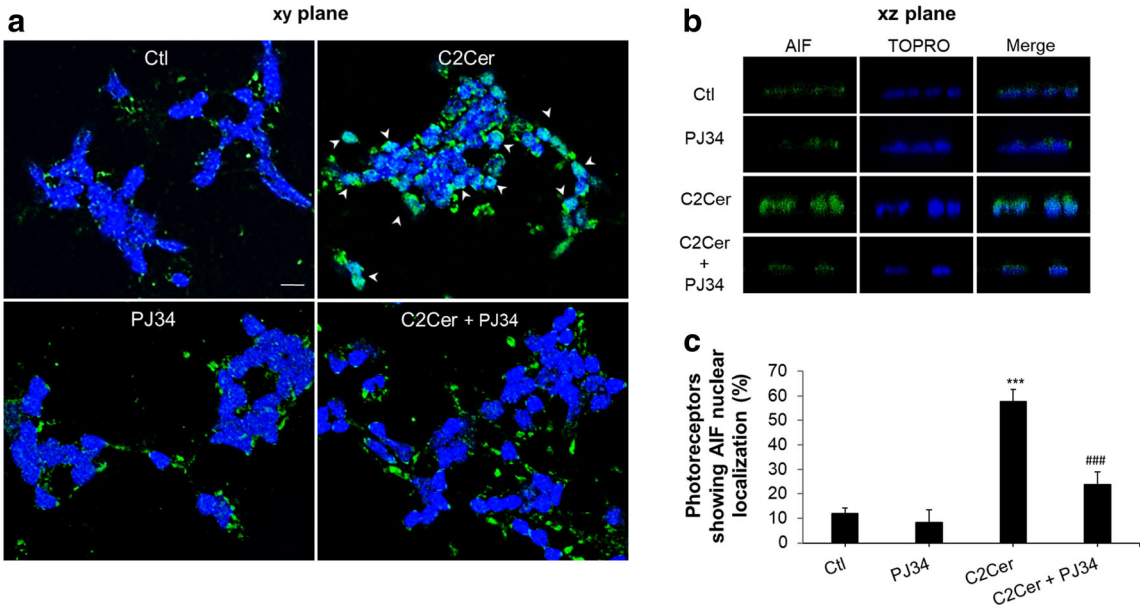

Fig. 6 C_2-Cer-induced nuclear translocation of AIF was prevented by inhibiting activation of PARP-1. Cultures were pretreated or not with PJ34 and then treated with vehicle or with C_2-Cer for 6 h. **a** Confocal photomicrographs in the xy plane show neuronal localization of AIF (green) and nuclear labeling with TOPRO-3 (blue); arrowheads show colocalization of AIF and TOPRO-3 labeling. Scale bar, 10 μm. **b** Confocal photomicrographs in the xz plane show localization of AIF (left column, green), nuclear labeling with TOPRO-3 (middle column, blue), and merge (right column). **c** Percentage of photoreceptors (mean ± SEM) showing AIF nuclear localization; $^{***}p < 0.001$, statistically significant differences compared to controls; $^{\#\#\#}p < 0.001$, statistically significant differences compared to C_2-Cer

with 10 μM C_2-Cer provokes the death of photoreceptors and amacrine neurons [5]. We now demonstrated that photoreceptors were more sensitive than amacrine neurons to C_2-Cer; a 6-h treatment with 10 μM C_2-Cer induced the selective death of photoreceptors, whereas amacrine neurons were virtually unaffected. This selectivity enabled us to investigate the intracellular mechanisms involved in Cer induction of photoreceptor death in culture. C_2-Cer induced a rapid and significant chromatin condensation and nuclear pyknosis in photoreceptors and provoked mitochondrial membrane depolarization. In addition, C_2-Cer promoted a rapid formation of ROS; increased ROS levels occurred early during C_2-Cer-elicited photoreceptor death. Multiple studies have demonstrated a close connection between Cer-induced cell death, loss of mitochondrial function and ROS production. We showed that a 24-h treatment with C_2-Cer leads to mitochondrial depolarization in photoreceptors [5]. Mitochondrial dysfunction is involved in Cer-induced death of cortical neurons and neuroblastoma cells [32, 33]. Cer enhances mitochondrial membrane permeability, thus leading to the release of pro-apoptotic mitochondrial proteins such as cytochrome c, Omi, and AIF and to the collapse of mitochondrial potential [34–38]. Cer affects mitochondrial membrane permeability indirectly, by promoting Bax translocation to mitochondria [39, 40] or acting synergistically with Bax to permeabilize mitochondrial outer membrane [41]. Early in vitro studies show Cer inhibits electron transport and induces formation of ROS in intact mitochondria, which are an early event in Cer-induced death; C_2-Cer inhibits several respiratory chain complexes [38, 42] and enhances ROS production [43]. C_2-Cer has been recently shown to increase ROS production in neuroblastoma cells [44].

Permeabilization of mitochondria is central to most pathways of programmed cell death. Activation of the apoptotic mitochondrial pathway is frequently associated to neuronal death, with the involvement of the caspase-9/caspase-3 cascade [32, 45]. Activated caspases are responsible for many of the characteristic features that usually define apoptotic cell death, such as the fragmentation of DNA detected by TUNEL labeling, which depends on a caspase-mediated DNA cleavage. However, our evidence suggests that activation of caspases was not involved in C_2-Cer-induced photoreceptor death. Treatment with C_2-Cer did not enhance TUNEL labeling in photoreceptors. No increase in the presence of cleaved caspase-3 in photoreceptors was observed in C_2-Cer-treated cultures, implying this caspase was not activated by C_2-Cer. In addition, z-VAD-FMK, a pan-caspase inhibitor, could not preclude C_2-Cer-induced photoreceptor death. Hence, our results suggest that Cer promoted photoreceptor death through a caspase-independent pathway. The involvement of caspases in photoreceptor death appears to be age and disease dependent. Caspases participate in apoptosis of photoreceptors early during development, in vivo and in vitro [46, 47]. Multiple proteases are involved in photoreceptor death in animal models of retina degeneration. Caspases are active in *rd* and *rds* mice [48], but their inhibition does not prevent photoreceptor degeneration [49]. Caspase-independent

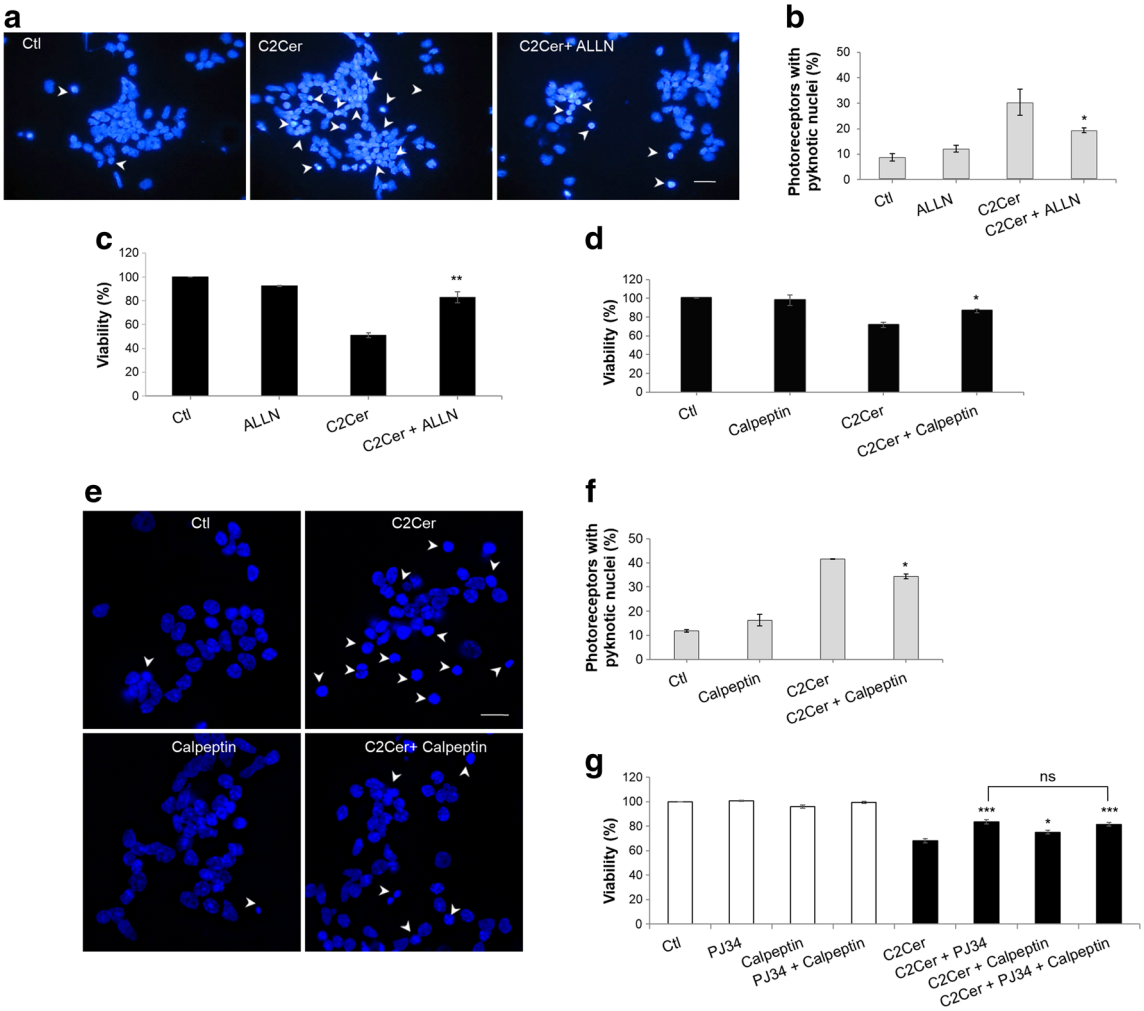

Fig. 7 Inhibition of calpain activity protected photoreceptors from C_2-Cer-induced death. Cultures were treated with vehicle or with C_2-Cer after pretreatment with 20 μM ALLN, a calpain and calpeptin inhibitor (**a**–**c**), 1 μM calpeptin, a calpain inhibitor (**d**–**f**) and 1 μM calpeptin + 1 μM PJ34 (**g**). **a**, **e** Photomicrographs show DAPI nuclear labeling of cultures pretreated with ALLN or Calpeptin, respectively, before C_2-Cer treatment; arrowheads indicate pyknotic nuclei. Scale bars, 10 μm. **b**, **f** Percentage of photoreceptors (mean ± SEM) having pyknotic nuclei. **c**, **d**, **g** Percentage of viability compared to controls (mean ± SEM) in cultures pretreated with ALLN, calpeptin, or calpeptin + PJ34 and then with vehicle or with C_2-Cer. $^*p < 0.05$, $^{**}p < 0.01$, $^{***}p < 0.001$, statistically significant differences compared to C_2-Cer

pathways and proteases other than caspases are also active participants in the demise of photoreceptors in retina degeneration [46, 48, 50]. Different cysteine proteases, including caspases, are activated in Cer-induced death of cone-like 661W cells [6].

PARP-1 activation has now emerged as the cornerstone of a distinctive mode of caspase-independent cell death named parthanatos [51–53]. PARP-1 plays opposing roles in cellular function. It has a vital role in DNA damage surveillance and repair, protecting cells against genotoxic stressors [54, 55]. Paradoxically, extensive DNA damage leads to an excessive PARP activation ultimately causing cell death. PARP-1 overactivation provokes NAD+ depletion and glycolysis inhibition, and the resulting energetic collapse leads to regulated necrosis [56, 57]. It also causes the massive formation of PAR polymers, with the consequent increase in protein poly(ADP ribosyl)ation (PARylation) [52] and the accumulation of PAR polymers in mitochondria, which leads to mitochondrial membrane depolarization and promotes the release and nuclear translocation of AIF [58, 59]. ROS can cause direct DNA damage, originating DNA strand breaks that are a frequent cause of PARP overactivation; hence, the early increase in ROS levels induced by C_2-Cer might promote PARP-1 overactivation. In concordance with this hypothesis, inhibition of PARP-1 was neuroprotective for photoreceptors. Pretreatment with two well-known PARP-1 inhibitors, PJ34 and BYK, increased cell viability upon C_2-Cer treatment; PJ34 prevented the increase in nuclear pyknosis induced by C_2-Cer. C_2-Cer augmented the formation of PAR polymers; a rapid and transient increase in the levels of PAR polymer

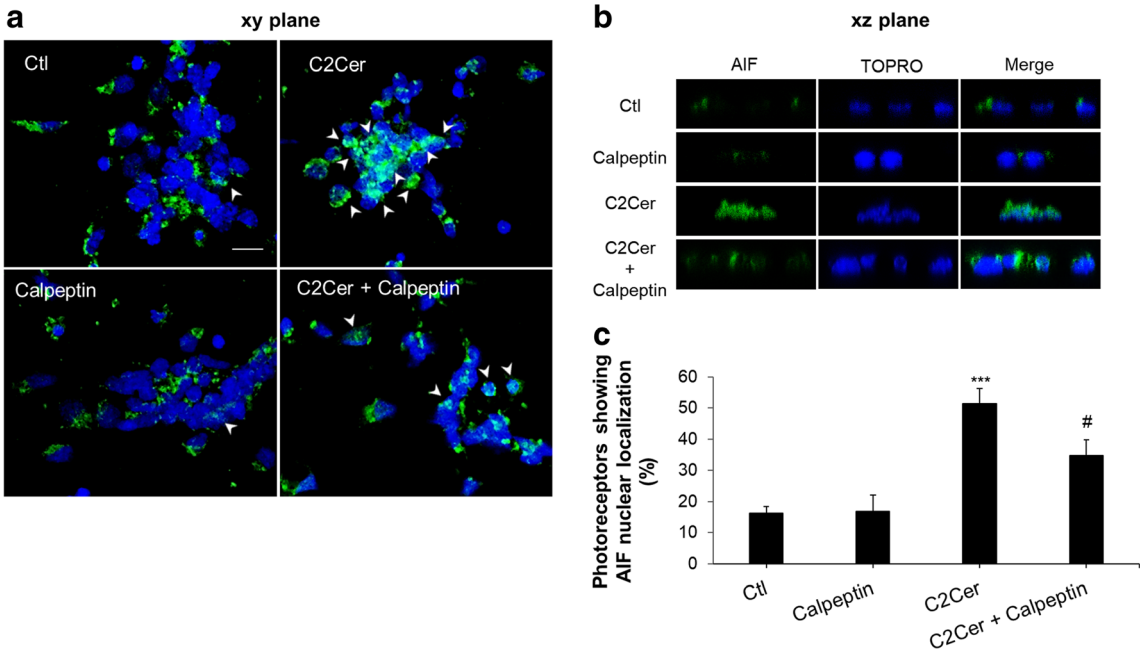

Fig. 8 Inhibiting calpain activation prevented C_2-Cer-induced AIF nuclear translocation. Cultures were pretreated or not with calpeptin and then treated with vehicle or with C_2-Cer for 6 h. **a** Confocal photomicrographs in the xy plane show neuronal localization of AIF (green) and nuclear labeling with TOPRO-3 (blue); arrowheads show colocalization of AIF and TOPRO-3 labeling. Scale bar, 10 μm. **b** Confocal photomicrographs in the xz plane show localization of AIF (left column, green), nuclear labeling with TOPRO-3 (middle column, blue), and merge (right column). **c** Percentage of photoreceptors (mean ± SEM) showing AIF nuclear localization. $^{***}p < 0.001$, statistically significant differences compared to controls; $^{\#}p < 0.05$, statistically significant differences compared to C_2-Cer

levels and in their expression in photoreceptors was observed in C_2-Cer -treated cultures, implying C_2-Cer enhanced protein PARylation. PAR levels result from the balance between the activities of PARP and polyADP ribose glycohydrolase, involved in PAR degradation; this enzyme might contribute to the decrease in PAR polymer levels observed after 2 h of C_2-Cer treatment. Noteworthy, the Western blot profile of PAR labeling, a unique, broad band, strikingly resembled that observed in rd1 retinas [60, 61] suggesting that retinal neurons might have a characteristic, retina-dependent, polyADP ribosylation pattern.

We previously demonstrated that oxidative stress induced photoreceptor death in culture by increasing the synthesis of Cer, including C16-Cer [5], which promotes cell death in several cell types [62, 63]. We now showed that treatment with C16-Cer, a biological Cer, with a longer acyl chain and different biophysical properties to that of C_2-Cer, also induced neuronal death and inhibiting PARP-1 activation reduced this death. As a whole, these findings support the involvement of PARP-1 activation in Cer-induced photoreceptor death. PARP-1 inhibition has been shown to ameliorate ischemia-reperfusion damage in the inner retina [64], to provide partial neuroprotection against NMDA-induced ganglion cell loss [65] and to prevent photoreceptor apoptosis induced by N-methyl-N-nitrosourea injection in rats [66]. Increased retinal PARP activity and protein PARylation are present in retinas of *rd1* and *rd2* mice, animal models of retina degeneration, and PARP-1 inhibition increases photoreceptor survival in both *rd1* and *rd2* retinas [60, 61, 67]. As described above, Cer is an arbitrator of cell death in these models. Our results link for the first time Cer-induced photoreceptor death to the activation of PARP-1 in these cells (Fig. 9). Although several works have demonstrated Cer induces PARP-1 cleavage [68–71], to our knowledge Cer-induced death has only been associated with PARP-1 activation followed by PAR accumulation and AIF release in neuroblastoma cells [72]. Hence, our results support the inclusion of PARP-1 activation among the cell death routines triggered by Cer.

Our results also evidence that PARP-1 activation provoked by C_2-Cer led to AIF nuclear translocation in photoreceptors. C_2-Cer enhanced AIF release from mitochondria, increasing its presence in photoreceptor nuclei and augmenting nuclear pyknosis. Inhibition of PARP-1 markedly prevented AIF nuclear translocation, reducing nuclear pyknosis. AIF, a bifunctional oxidoreductase that functions as both a ROS scavenger in oxidative phosphorylation and an apoptogenic molecule, is anchored to the mitochondrial inner membrane, with vital functions in bioenergetics. Different insults promote its cleavage and release to the cytosol followed by its translocation to the nucleus, where it induces DNA fragmentation [23, 73]. In the retina, AIF is usually localized in the inner segments of photoreceptors, which contain mitochondria and endoplasmic reticulum [74]. PARP-1 overactivation is known to promote AIF release from mitochondria and its subsequent nuclear

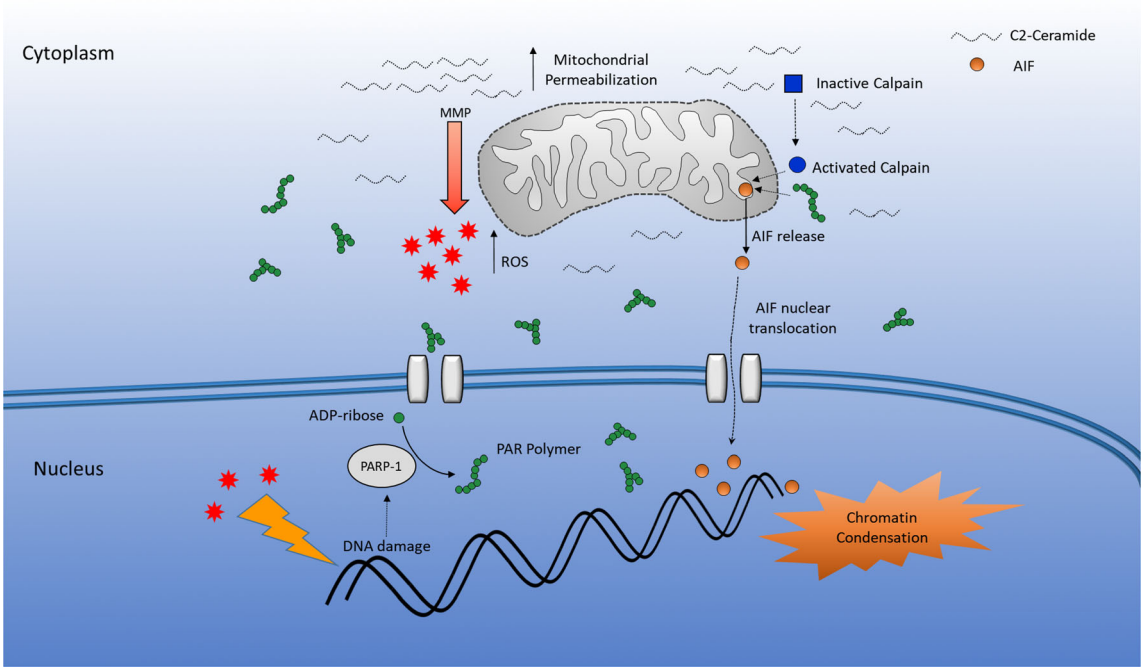

Fig. 9 C_2-Cer unleashes parthanatos to elicit a rapid photoreceptor death. C_2-Cer induces mitochondrial dysfunction in photoreceptors, enhancing the formation of ROS, which lead to DNA damage. This damage brings about the activation of PARP-1, promoting the polymerization of ADP-ribose and resulting in the excessive synthesis of PAR polymers, which diffuse to the cytoplasm and mitochondria and can further affect mitochondrial membrane permeabilization, decreasing mitochondrial membrane potential (MMP) and causing AIF release. In addition, C_2-Cer causes activation of calpains, which also contribute to AIF release. AIF then translocates to the nuclei and provokes large-scale DNA fragmentation, irreversibly committing photoreceptors to death

translocation; PAR polymers diffuse from the nucleus to the mitochondria, where they bind to AIF and promote its nuclear translocation, resulting in a large scale DNA fragmentation [25, 58, 75, 76]. Excitotoxic damage induces ROS formation, which causes DNA damage and provokes the excessive PARP-1 activation and AIF-mediated cell death [58]. Similarly, C_2-Cer-induced increase in ROS levels in photoreceptors might cause DNA damage, promoting overactivation of PARP-1 and the resulting increase in PAR polymers, which might in turn lead to AIF translocation and the subsequent photoreceptor pyknosis (Fig. 9). Hence, PARP-1 activation and the resulting AIF translocation might be the key events setting off a cell death cascade in photoreceptors, acting as caspase-independent death effectors.

Calpains and cathepsins have also been shown to participate in AIF release [28, 77, 78]. Calpains are calcium-dependent cysteine proteases that may trigger caspase-independent cell death pathways. Both calpains and cathepsins participate in photoreceptor death after Cer treatment or in the *rd1* retina [6, 48]. Inhibiting calpain activity with ALLN and calpeptin reduced neuronal death induced by C_2-Cer, decreasing photoreceptor nuclear pyknosis. Calpain inhibition with calpeptin also decreased AIF nuclear translocation. This suggests that C_2-Cer activated calpains to provoke photoreceptor death and this activation contributed to AIF translocation. In contrast, two different cathepsin inhibitors showed no protective effect. Noteworthy, ALLN, a broad-spectrum protease inhibitor that inhibits calpains, cathepsins, and the proteasome [79] was more effective than calpeptin at preserving photoreceptor viability. This is consistent with previous reports that general protease inhibitors are more effective at precluding AIF release than more specific inhibitors [27] and suggests that several cysteine proteases might participate in AIF cleavage. Although the involvement of other proteases cannot be ruled out, our data support calpains participate in AIF release and subsequent photoreceptor death.

The sequential activation of PARP-1 and calpains play a role in necrotic programmed cell death [80]. Evaluation of the effect of the combined treatment with a PARP-1 (PJ34) and a calpain (calpeptin) inhibitor evidenced the same protection as either of them by itself, with no additive or synergic effect. This implies that either PARP-1 is activated upstream of calpain activation or both PARP-1 and calpain share a downstream pathway leading to photoreceptor death (Fig. 9).

Cer has been involved in the initiation of necroptosis and autophagy [12, 81] and caspase-independent, cell death programs in which PARP-1 activation has also been implicated. The sequential activation of PARP-1, calpains, and Bax may play a role in necrotic programmed cell death [80] and PARP-1 activation and PAR polymer accumulation have been

postulated to regulate necroptosis [82, 83]. Necroptosis leads to cell death with some of the morphological characteristics of necrosis, such as the loss of plasma membrane integrity, through the activation of a program orchestrated by RIPK1 and inhibited by necrostatin [84]. Our results evidence C_2-Cer did not induce the loss of plasma membrane integrity, as determined by the absence of LDH leakage; in addition, necrostatin, the selective RIPK1 inhibitor could not preserve photoreceptor viability, ruling out programmed necrosis as a cell death program activated by C_2-Cer in photoreceptors. PARP-1 has also been proposed to participate in autophagy [85], which is usually a protective pathway, oriented at preserving cell viability upon situations such as trophic factor or nutrient withdrawal. Autophagy might either contribute to C_2-Cer-induced photoreceptor death or have a protective role upon C_2-Cer treatment. In this context, a dual role for PARP-1 has been shown in the modulation of parthanatos and autophagy upon oxidative stress, activating both parthanatos and a pro-survival autophagy [30]. Pretreatment with 3-MA and Bafilomycin A1, which inhibit autophagosome formation and the late phase of autophagy, respectively, did neither prevent nor enhance photoreceptor death. This suggests that autophagy neither contributed to C_2-Cer-induced death nor had a protective role upon C_2-Cer treatment.

In conclusion, our results strongly support a novel mechanism for Cer-induced death of retina photoreceptors, involving PARP-1 overactivation, increased PAR formation, calpain activation, subsequent AIF release from mitochondria, and DNA degradation. This Cer-elicited pathway may be of relevance both from the perspective of pathogenesis and in the search of molecular targets for treating these diseases since the increased levels of Cer and PARP can contribute to advance or exacerbate neuroinflammation [86] even in the absence of photoreceptor death.

Acknowledgements N. P. Rotstein and L.E. Politi are principal researchers from the National Research Council of Argentina (CONICET) and Professors of Biological Chemistry and Cell Biology, respectively, from the Universidad Nacional del Sur (UNS). F.H. Prado Spalm, M.S. Vera, and M.J. Dibo are Doctoral Research fellows and M.V. Simon is an Assistant Researcher from CONICET. Funds are from the National Agency for Science and Technology (ANPCYT) (PICT-2015-0284 to NPR); National Research Council of Argentina (CONICET) (PIP 11220-1101–00827, to LEP and NPR); and the Secretary of Science and Technology, Universidad Nacional del Sur (to NPR).

The authors are grateful to E. Beatriz de los Santos and Edgardo Buzzi for their expert technical assistance.

Authors' Contribution Facundo Prado Spalm is responsible for planning, conducting, evaluating, and interpreting the experiments and manuscript writing. Marcela Vera is responsible for conducting and evaluating the experiments and manuscript revision. M. Victoria Simón is responsible for conducting and evaluating the experiments and manuscript revision. Luis Politi is responsible for evaluating and interpreting the experiments and manuscript revision. Nora Rotstein is responsible for planning, evaluating, and interpreting the experiments and manuscript writing.

Compliance with Ethical Standards

Conflict of Interest The authors declare that they have no conflict of interest.

References

1. Hartong DT, Berson EL, Dryja TP (2006) Retinitis pigmentosa. Lancet 368:1795–1809. https://doi.org/10.1016/S0140-6736(06)69740-7
2. Hannun YA, Obeid LM (2008) Principles of bioactive lipid signalling: lessons from sphingolipids. Nat Rev Mol Cell Biol 9:139–150. https://doi.org/10.1038/nrm2329
3. Rotstein NP, Miranda GE, Abrahan CE, German OL (2010) Regulating survival and development in the retina: key roles for simple sphingolipids. J Lipid Res 51:1247–1262. https://doi.org/10.1194/jlr.R003442
4. Young MM, Kester M, Wang H-G (2013) Sphingolipids: regulators of crosstalk between apoptosis and autophagy. J Lipid Res 54:5–19. https://doi.org/10.1194/jlr.R031278
5. German OL, Miranda GE, Abrahan CE, Rotstein NP (2006) Ceramide is a mediator of apoptosis in retina photoreceptors. Invest Ophthalmol Vis Sci 47:1658–1668. https://doi.org/10.1167/iovs.05-1310
6. Sanvicens N, Cotter TG (2006) Ceramide is the key mediator of oxidative stress-induced apoptosis in retinal photoreceptor cells. J Neurochem 98:1432–1444. https://doi.org/10.1111/j.1471-4159.2006.03977.x
7. Ranty M-L, Carpentier S, Cournot M, Rico-Lattes I, Malecaze F, Levade T, Delisle M-B, Quintyn J-C (2009) Ceramide production associated with retinal apoptosis after retinal detachment. Graefes Arch Clin Exp Ophthalmol 247:215–224. https://doi.org/10.1007/s00417-008-0957-6
8. Fan J, Wu BX, Crosson CE (2016) Suppression of acid sphingomyelinase protects the retina from ischemic injury. Investig Opthalmol Vis Sci 57:4476–4484. https://doi.org/10.1167/iovs.16-19717
9. Strettoi E, Gargini C, Novelli E, Sala G, Piano I, Gasco P, Ghidoni R (2010) Inhibition of ceramide biosynthesis preserves photoreceptor structure and function in a mouse model of retinitis pigmentosa. Proc Natl Acad Sci U S A 107:18706–18711. https://doi.org/10.1073/pnas.1007644107
10. Chen H, Tran J-TA, Eckerd A, Huynh T-P, Elliott MH, Brush RS, Mandal NA (2013) Inhibition of de novo ceramide biosynthesis by FTY720 protects rat retina from light-induced degeneration. J Lipid Res 54:1616–1629. https://doi.org/10.1194/jlr.M035048
11. Stiles M, Qi H, Sun E, Tan J, Porter H, Allegood J, Chalfant CE, Yasumura D et al (2016) Sphingolipid profile alters in retinal dystrophic P23H-1 rats and systemic FTY720 can delay retinal degeneration. J Lipid Res 57:818–831. https://doi.org/10.1194/jlr.M063719
12. Scarlatti F, Bauvy C, Ventruti A, Sala G, Cluzeaud F, Vandewalle A, Ghidoni R, Codogno P (2004) Ceramide-mediated macroautophagy involves inhibition of protein kinase B and up-regulation of beclin 1. J Biol Chem 279:18384–18391. https://doi.org/10.1074/jbc.M313561200
13. Sims K, Haynes CA, Kelly S, Allegood JC, Wang E, Momin A, Leipelt M, Reichart D et al (2010) Kdo2-lipid A, a TLR4-specific agonist, induces de novo sphingolipid biosynthesis in RAW264.7 macrophages, which is essential for induction of autophagy. J Biol Chem 285:38568–38579. https://doi.org/10.1074/jbc.M110.170621

14. Saddoughi SA, Gencer S, Peterson YK, Ward KE, Mukhopadhyay A, Oaks J, Bielawski J, Szulc ZM et al (2013) Sphingosine analogue drug FTY720 targets I2PP2A/SET and mediates lung tumour suppression via activation of PP2A-RIPK1-dependent necroptosis. EMBO Mol Med 5:105–121. https://doi.org/10.1002/emmm.201201283
15. Politi LE, Lehar M, Adler R (1988) Development of neonatal mouse retinal neurons and photoreceptors in low density cell culture. Invest Ophthalmol Vis Sci 29:534–543
16. Adler R (1982) Regulation of neurite growth in purified retina neuronal cultures: effects of PNPF, a substratum-bound, neurite-promoting factor. J Neurosci Res 8:165–177. https://doi.org/10.1002/jnr.490080207
17. Ji L, Zhang G, Uematsu S, Akahori Y, Hirabayashi Y (1995) Induction of apoptotic DNA fragmentation and cell death by natural ceramide. FEBS Lett 358:211–214. https://doi.org/10.1016/0014-5793(94)01428-4
18. Jordán J, Galindo MF, Prehn JH, Weichselbaum RR, Beckett M, Ghadge GD, Roos RP, Leiden JM et al (1997) P53 expression induces apoptosis in hippocampal pyramidal neuron cultures. J Neurosci 17:1397–1405. https://doi.org/10.1523/JNEUROSCI.17-04-01397.1997
19. Mosmann T (1983) Rapid colorimetric assay for cellular growth and survival: application to proliferation and cytotoxicity assays. J Immunol Methods 65:55–63. https://doi.org/10.1016/0022-1759(83)90303-4
20. Rotstein NP, Politi LE, German OL, Girotti R (2003) Protective effect of docosahexaenoic acid on oxidative stress-induced apoptosis of retina photoreceptors. Investig Ophthalmol Vis Sci 44:2252–2259. https://doi.org/10.1167/iovs.02-0901
21. Sánchez Campos S, Rodríguez Diez G, Oresti GM, Salvador GA (2015) Dopaminergic neurons respond to iron-induced oxidative stress by modulating lipid acylation and deacylation cycles. PLoS One 10:1–20. https://doi.org/10.1371/journal.pone.0130726
22. Laemmli UK (1970) Cleavage of structural proteins during the assembly of the head of bacteriophage T4. Nature 227:680–685. https://doi.org/10.1038/227680a0
23. Susin SA, Lorenzo HK, Zamzami N, Marzo I, Snow BE, Brothers GM, Mangion J, Jacotot E et al (1999) Molecular characterization of mitochondrial apoptosis-inducing factor. Nature 397:441–446. https://doi.org/10.1038/17135
24. Ruchalski K, Mao H, Li Z, Wang Z, Gillers S, Wang Y, Mosser DD, Gabai V et al (2006) Distinct hsp70 domains mediate apoptosis-inducing factor release and nuclear accumulation. J Biol Chem 281:7873–7880. https://doi.org/10.1074/jbc.M513728200
25. Yu S-W, Andrabi SA, Wang H, Kim NS, Poirier GG, Dawson TM, Dawson VL (2006) Apoptosis-inducing factor mediates poly(ADP-ribose) (PAR) polymer-induced cell death. Proc Natl Acad Sci 103:18314–18319. https://doi.org/10.1073/pnas.0606528103
26. Wang Y, Kim NS, Li X, Greer PA, Koehler RC, Dawson VL, Dawson TM (2009) Calpain activation is not required for AIF translocation in PARP-1-dependent cell death (parthanatos). J Neurochem 110:687–696. https://doi.org/10.1111/j.1471-4159.2009.06167.x
27. Yuste VJ, Moubarak RS, Delettre C, Bras M, Sancho P, Robert N, d'Alayer J, Susin SA (2005) Cysteine protease inhibition prevents mitochondrial apoptosis-inducing factor (AIF) release. Cell Death Differ 12:1445–1448. https://doi.org/10.1038/sj.cdd.4401687
28. Polster BM, Basañez G, Etxebarria A, Hardwick JM, Nicholls DG (2005) Calpain I induces cleavage and release of apoptosis-inducing factor from isolated mitochondria. J Biol Chem 280:6447–6454. https://doi.org/10.1074/jbc.M413269200
29. Douglas DL, Baines CP (2014) PARP1-mediated necrosis is dependent on parallel JNK and Ca^{2+}/calpain pathways. J Cell Sci 127:4134–4145. https://doi.org/10.1242/jcs.128009
30. Jiang H-Y, Yang Y, Zhang Y-Y, Xie Z, Zhao X-Y, Sun Y, Kong W-J (2018) The dual role of poly(ADP-ribose) polymerase-1 in modulating parthanatos and autophagy under oxidative stress in rat cochlear marginal cells of the stria vascularis. Redox Biol 14:361–370. https://doi.org/10.1016/j.redox.2017.10.002
31. Piano I, Novelli E, Gasco P, Ghidoni R, Strettoi E, Gargini C (2013) Cone survival and preservation of visual acuity in an animal model of retinal degeneration. Eur J Neurosci 37:1853–1862. https://doi.org/10.1111/ejn.12196
32. Stoica BA, Movsesyan VA, Lea PM, Faden AI (2003) Ceramide-induced neuronal apoptosis is associated with dephosphorylation of Akt, BAD, FKHR, GSK-3beta, and induction of the mitochondrial-dependent intrinsic caspase pathway. Mol Cell Neurosci 22:365–382. https://doi.org/10.1016/S1044-7431(02)00028-3
33. Kim NH, Kim K, Park WS, Son HS, Bae Y (2007) PKB/Akt inhibits ceramide-induced apoptosis in neuroblastoma cells by blocking apoptosis-inducing factor (AIF) translocation. J Cell Biochem 102:1160–1170. https://doi.org/10.1002/jcb.21344
34. Siskind LJ, Kolesnick RN, Colombini M (2002) Ceramide channels increase the permeability of the mitochondrial outer membrane to small proteins. J Biol Chem 277:26796–26803. https://doi.org/10.1074/jbc.M200754200
35. Siskind LJ, Davoody A, Lewin N, Marshall S, Colombini M (2003) Enlargement and contracture of C2-ceramide channels. Biophys J 85:1560–1575. https://doi.org/10.1016/S0006-3495(03)74588-3
36. Stoica BA, Movsesyan VA, Knoblach SM, Faden AI (2005) Ceramide induces neuronal apoptosis through mitogen-activated protein kinases and causes release of multiple mitochondrial proteins. Mol Cell Neurosci 29:355–371. https://doi.org/10.1016/j.mcn.2005.02.009
37. Colombini M (2010) Ceramide channels and their role in mitochondria-mediated apoptosis. Biochim Biophys Acta 1797:1239–1244. https://doi.org/10.1016/j.bbabio.2010.01.021
38. Di Paola M, Cocco T, Lorusso M (2000) Ceramide interaction with the respiratory chain of heart mitochondria †. Biochemistry 39:6660–6668. https://doi.org/10.1021/bi9924415
39. Pettus BJ, Chalfant CE, Hannun YA (2002) Ceramide in apoptosis: an overview and current perspectives. Biochim Biophys Acta Mol Cell Biol Lipids 1585:114–125. https://doi.org/10.1016/S1388-1981(02)00331-1
40. Bidère N, Lorenzo HK, Carmona S, Laforge M, Harper F, Dumont C, Senik A (2003) Cathepsin D triggers Bax activation, resulting in selective apoptosis-inducing factor (AIF) relocation in T lymphocytes entering the early commitment phase to apoptosis. J Biol Chem 278:31401–31411. https://doi.org/10.1074/jbc.M301911200
41. Ganesan V, Perera MN, Colombini D, Datskovskiy D, Chadha K, Colombini M (2010) Ceramide and activated Bax act synergistically to permeabilize the mitochondrial outer membrane. Apoptosis 15:553–562. https://doi.org/10.1007/s10495-009-0449-0
42. Gudz TI, Tserng KY, Hoppel CL (1997) Direct inhibition of mitochondrial respiratory chain complex III by cell-permeable ceramide. J Biol Chem 272:24154–24158. https://doi.org/10.1074/jbc.272.39.24154
43. García-Ruiz C, Colell A, Marí M, Morales A, Fernández-Checa JC (1997) Direct effect of ceramide on the mitochondrial electron transport chain leads to generation of reactive oxygen species. Role of mitochondrial glutathione. J Biol Chem 272:11369–11377. https://doi.org/10.1074/jbc.272.17.11369
44. Fan C, Liu Y, Zhao M, Zhan R, Cui W, Jin H, Teng Y, Lv P et al (2017) Autophagy inhibits C2-ceramide-mediated cell death by decreasing the reactive oxygen species levels in SH-SY5Y cells. Neurosci Lett 651:198–206. https://doi.org/10.1016/j.neulet.2017.03.006
45. Falluel-Morel A, Aubert N, Vaudry D, Basille M, Fontaine M, Fournier A, Vaudry H, Gonzalez BJ (2004) Opposite regulation of the mitochondrial apoptotic pathway by C2-ceramide and

PACAP through a MAP-kinase-dependent mechanism in cerebellar granule cells. J Neurochem 91:1231–1243. https://doi.org/10.1111/j.1471-4159.2004.02810.x
46. Donovan M, Cotter TG (2002) Caspase-independent photoreceptor apoptosis in vivo and differential expression of apoptotic protease activating factor-1 and caspase-3 during retinal development. Cell Death Differ 9:1220–1231. https://doi.org/10.1038/sj.cdd.4401105
47. Donovan M, Doonan F, Cotter TG (2006) Decreased expression of pro-apoptotic Bcl-2 family members during retinal development and differential sensitivity to cell death. Dev Biol 291:154–169. https://doi.org/10.1016/j.ydbio.2005.12.026
48. Lohr HR, Kuntchithapautham K, Sharma AK, Rohrer B (2006) Multiple, parallel cellular suicide mechanisms participate in photoreceptor cell death. Exp Eye Res 83:380–389. https://doi.org/10.1016/j.exer.2006.01.014
49. Yoshizawa K, Kiuchi K, Nambu H, Yang J, Senzaki H, Kiyozuka Y, Shikata N, Tsubura A (2002) Caspase-3 inhibitor transiently delays inherited retinal degeneration in C3H mice carrying the rd gene. Graefes Arch Clin Exp Ophthalmol 240:214–219. https://doi.org/10.1007/s00417-002-0427-5
50. Doonan F, Donovan M, Cotter TG (2005) Activation of multiple pathways during photoreceptor apoptosis in the rd mouse. Invest Ophthalmol Vis Sci 46:3530–3538. https://doi.org/10.1167/iovs.05-0248
51. Galluzzi L, Vitale I, Abrams JM, Alnemri ES, Baehrecke EH, Blagosklonny MV, Dawson TM, Dawson VL et al (2012) Molecular definitions of cell death subroutines: recommendations of the nomenclature committee on cell death 2012. Cell Death Differ 19:107–120. https://doi.org/10.1038/cdd.2011.96
52. Andrabi SA, Dawson TM, Dawson VL (2008) Mitochondrial and nuclear cross talk in cell death: parthanatos. Ann N Y Acad Sci 1147:233–241. https://doi.org/10.1196/annals.1427.014
53. Narne P, Pandey V, Simhadri PK, Phanithi PB (2017) Poly(ADP-ribose)polymerase-1 hyperactivation in neurodegenerative diseases: the death knell tolls for neurons. Semin Cell Dev Biol 63:154–166. https://doi.org/10.1016/j.semcdb.2016.11.007
54. Hong SJ, Dawson TM, Dawson VL (2004) Nuclear and mitochondrial conversations in cell death: PARP-1 and AIF signaling. Trends Pharmacol Sci 25:259–264. https://doi.org/10.1016/j.tips.2004.03.005
55. Schreiber V, Amé J-C, Dollé P, Schultz I, Rinaldi B, Fraulob V, Ménissier-de Murcia J, de Murcia G (2002) Poly(ADP-ribose) polymerase-2 (PARP-2) is required for efficient base excision DNA repair in association with PARP-1 and XRCC1. J Biol Chem 277:23028–23036. https://doi.org/10.1074/jbc.M202390200
56. Ying W, Garnier P, Swanson RA (2003) NAD+ repletion prevents PARP-1-induced glycolytic blockade and cell death in cultured mouse astrocytes. Biochem Biophys Res Commun 308:809–813. https://doi.org/10.1016/S0006-291X(03)01483-9
57. Andrabi SA, Umanah GKE, Chang C, Stevens DA, Karuppagounder SS, Gagné J-P, Poirier GG, Dawson VL et al (2014) Poly(ADP-ribose) polymerase-dependent energy depletion occurs through inhibition of glycolysis. Proc Natl Acad Sci U S A 111:10209–10214. https://doi.org/10.1073/pnas.1405158111
58. Wang Y, Dawson VL, Dawson TM (2009) Poly(ADP-ribose) signals to mitochondrial AIF: a key event in parthanatos. Exp Neurol 218:193–202. https://doi.org/10.1016/j.expneurol.2009.03.020
59. Baek S-H, Bae O-N, Kim E-K, Yu S-W (2013) Induction of mitochondrial dysfunction by poly(ADP-ribose) polymer: implication for neuronal cell death. Mol Cell 36:258–266. https://doi.org/10.1007/s10059-013-0172-0
60. Paquet-Durand F, Silva J, Talukdar T, Johnson LE, Azadi S, van Veen T, Ueffing M, Hauck SM et al (2007) Excessive activation of poly(ADP-ribose) polymerase contributes to inherited photoreceptor degeneration in the retinal degeneration 1 mouse. J Neurosci 27:10311–10319. https://doi.org/10.1523/JNEUROSCI.1514-07.2007
61. Sahaboglu A, Sharif A, Feng L, Secer E, Zrenner E, Paquet-Durand F (2017) Temporal progression of PARP activity in the Prph2 mutant rd2 mouse: neuroprotective effects of the PARP inhibitor PJ34. PLoS One 12:e0181374. https://doi.org/10.1371/journal.pone.0181374
62. Stiban J, Perera M (2015) Very long chain ceramides interfere with C16-ceramide-induced channel formation: a plausible mechanism for regulating the initiation of intrinsic apoptosis. Biochim Biophys Acta Biomembr 1848:561–567. https://doi.org/10.1016/j.bbamem.2014.11.018
63. Hernández-Corbacho MJ, Canals D, Adada MM, Liu M, Senkal CE, Yi JK, Mao C, Luberto C et al (2015) Tumor necrosis factor-α (TNFα)-induced ceramide generation via ceramide synthases regulates loss of focal adhesion kinase (FAK) and programmed cell death. J Biol Chem 290:25356–25373. https://doi.org/10.1074/jbc.M115.658658
64. Chiang SK, Lam TT (2000) Post-treatment at 12 or 18 hours with 3-aminobenzamide ameliorates retinal ischemia-reperfusion damage. Invest Ophthalmol Vis Sci 41:3210–3214
65. Goebel DJ, Winkler BS (2006) Blockade of PARP activity attenuates poly(ADP-ribosyl)ation but offers only partial neuroprotection against NMDA-induced cell death in the rat retina. J Neurochem 98:1732–1745. https://doi.org/10.1111/j.1471-4159.2006.04065.x
66. Miki K, Uehara N, Shikata N, Matsumura M, Tsubura A (2007) Poly (ADP-ribose) polymerase inhibitor 3-aminobenzamide rescues N-methyl-N-nitrosourea-induced photoreceptor cell apoptosis in Sprague-Dawley rats through preservation of nuclear factor-kappaB activity. Exp Eye Res 84:285–292. https://doi.org/10.1016/j.exer.2006.09.023
67. Sahaboglu A, Barth M, Secer E, del Amo EM, Urtti A, Arsenijevic Y, Zrenner E, Paquet-Durand F (2016) Olaparib significantly delays photoreceptor loss in a model for hereditary retinal degeneration. Sci Rep 6:39537. https://doi.org/10.1038/srep39537
68. Spinedi A, Amendola A, Di Bartolomeo S, Piacentini M (1998) Ceramide-induced apoptosis is mediated by caspase activation independently from retinoblastoma protein post-translational modification. Biochem Biophys Res Commun 243:852–857. https://doi.org/10.1006/bbrc.1998.8184
69. Flowers M, Fabriás G, Delgado A, Casas J, Abad JL, Cabot MC (2012) C6-ceramide and targeted inhibition of acid ceramidase induce synergistic decreases in breast cancer cell growth. Breast Cancer Res Treat 133:447–458. https://doi.org/10.1007/s10549-011-1768-8
70. Kota V, Dhople VM, Fullbright G, Smythe NM, Szulc ZM, Bielawska A, Hama H (2013) 2′-Hydroxy C16-ceramide induces apoptosis-associated proteomic changes in C6 glioma cells. J Proteome Res 12:4366–4375. https://doi.org/10.1021/pr4003432
71. Xu R, Wang K, Mileva I, Hannun YA, Obeid LM, Mao C (2016) Alkaline ceramidase 2 and its bioactive product sphingosine are novel regulators of the DNA damage response. Oncotarget 7:18440–18457. https://doi.org/10.18632/oncotarget.7825
72. Czubowicz K, Strosznajder R (2014) Ceramide in the molecular mechanisms of neuronal cell death. The role of sphingosine-1-phosphate. Mol Neurobiol 50:26–37. https://doi.org/10.1007/s12035-013-8606-4
73. Otera H, Ohsakaya S, Nagaura Z-I, Ishihara N, Mihara K (2005) Export of mitochondrial AIF in response to proapoptotic stimuli depends on processing at the intermembrane space. EMBO J 24:1375–1386. https://doi.org/10.1038/sj.emboj.7600614
74. Sanges D, Comitato A, Tammaro R, Marigo V (2006) Apoptosis in retinal degeneration involves cross-talk between apoptosis-inducing factor (AIF) and caspase-12 and is blocked by calpain inhibitors. Proc Natl Acad Sci 103:17366–17371. https://doi.org/10.1073/pnas.0606276103
75. Andrabi SA, Kim NS, Yu S-W, Wang H, Koh DW, Sasaki M, Klaus JA, Otsuka T et al (2006) Poly(ADP-ribose) (PAR) polymer is a

death signal. Proc Natl Acad Sci 103:18308–18313. https://doi.org/10.1073/pnas.0606526103
76. Wang Y, Kim NS, Haince J-F, Kang HC, David KK, Andrabi SA, Poirier GG, Dawson VL et al (2011) Poly(ADP-ribose) (PAR) binding to apoptosis-inducing factor is critical for PAR polymerase-1-dependent cell death (parthanatos). Sci Signal 4:ra20. https://doi.org/10.1126/scisignal.2000902
77. Cao G, Xing J, Xiao X, Liou AKF, Gao Y, Yin X-M, Clark RSB, Graham SH et al (2007) Critical role of calpain I in mitochondrial release of apoptosis-inducing factor in ischemic neuronal injury. J Neurosci 27:9278–9293. https://doi.org/10.1523/JNEUROSCI.2826-07.2007
78. Yang Q, Zhang C, Wei H, Meng Z, Li G, Xu Y, Chen Y (2017) Caspase-independent pathway is related to nilotinib cytotoxicity in cultured cardiomyocytes. Cell Physiol Biochem 42:2182–2193. https://doi.org/10.1159/000479993
79. Czerwinski A, Basava C, Dauter M, Dauter Z (2015) Crystal structure of N-{N-[N-acetyl-(S)-leuc-yl]-(S)-leuc-yl}norleucinal (ALLN), an inhibitor of proteasome. Acta Crystallogr Sect E Crystallogr Commun 71:254–257. https://doi.org/10.1107/S2056989015002091
80. Moubarak RS, Yuste VJ, Artus C, Bouharrour A, Greer PA, Menissier-de Murcia J, Susin SA (2007) Sequential activation of poly(ADP-ribose) polymerase 1, calpains, and Bax is essential in apoptosis-inducing factor-mediated programmed necrosis. Mol Cell Biol 27:4844–4862. https://doi.org/10.1128/MCB.02141-06
81. Bailey LJ, Alahari S, Tagliaferro A, Post M, Caniggia I (2017) Augmented trophoblast cell death in preeclampsia can proceed via ceramide-mediated necroptosis. Cell Death Dis 8:e2590–e2590. https://doi.org/10.1038/cddis.2016.483
82. Jouan-Lanhouet S, Arshad MI, Piquet-Pellorce C, Martin-Chouly C, Le Moigne-Muller G, Van Herreweghe F, Takahashi N, Sergent O et al (2012) TRAIL induces necroptosis involving RIPK1/RIPK3-dependent PARP-1 activation. Cell Death Differ 19:2003–2014. https://doi.org/10.1038/cdd.2012.90
83. Aredia F, Scovassi AI (2014) Involvement of PARPs in cell death. Front Biosci (Elite Ed) 6:308–317
84. Vandenabeele P, Galluzzi L, Vanden Berghe T, Kroemer G (2010) Molecular mechanisms of necroptosis: an ordered cellular explosion. Nat Rev Mol Cell Biol 11:700–714. https://doi.org/10.1038/nrm2970
85. Aredia F, Scovassi AI (2014) Poly(ADP-ribose): a signaling molecule in different paradigms of cell death. Biochem Pharmacol 92:157–163. https://doi.org/10.1016/j.bcp.2014.06.021
86. Morris G, Walker AJ, Berk M, Maes M, Puri BK (2017) Cell death pathways: a novel therapeutic approach for neuroscientists. Mol Neurobiol 55:5767–5786. https://doi.org/10.1007/s12035-017-0793-y